UCRL 8710

UNIVERSITY OF
CALIFORNIA

Ernest O. Lawrence

Radiation Laboratory

INDEPENDENT YIELDS OF ISOMERIC PAIRS IN NUCLEAR REACTIONS

BERKELEY, CALIFORNIA

DISCLAIMER

UCRL-8710
Chemistry-General

UNIVERSITY OF CALIFORNIA

Lawrence Radiation Laboratory
Berkeley, California

Contract No. W-7405-eng-48

INDEPENDENT YIELDS OF ISOMERIC PAIRS IN NUCLEAR REACTIONS

Sylvia Mae Bailey

(Thesis)

April 1959

Printed for the U. S. Atomic Energy Commission

Printed in USA. Price $2.25. Available from the
Office of Technical Services
U. S. Department of Commerce
Washington 25, D. C.

INDEPENDENT YIELDS OF ISOMERIC PAIRS IN NUCLEAR REACTIONS

Contents

INDEPENDENT YIELDS OF ISOMERIC PAIRS IN NUCLEAR REACTIONS

Sylvia Mae Bailey

Lawrence Radiation Laboratory and Department of Chemistry
University of California, Berkeley, California

April 1959

ABSTRACT

The Cd^{115m} and Cd^{115} isomers produced in 12- to 340-Mev proton bombardments of U^{238} were isolated by radiochemical methods. The cumulative yield ratios of Cd^{115}/Cd^{115m} were determined. In the 45-Mev helium-ion fission of uranium, an estimation of the independent-yield ratio of Pm^{148} (5.3-day) to Pm^{148} (43-day) was made. In the deuteron fission of uranium at about 20 Mev, an estimate of the independent-yield ratio of Nb^{95m} to the total niobium of mass 95 was made. A literature survey on experimental isomer ratios from fission was made.

The yield ratio of Sc^{44m}/Sc^{44} was measured in $Sc^{45}(\alpha,\alpha n)Sc^{44}$ reactions with helium ions of energies between 20 and 43 Mev and at 320 Mev. The Sc^{44m}/Sc^{44} ratio was measured in $K^{41}(\alpha,n)Sc^{44}$ reactions at 10 and 13 Mev.

The compound-nucleus model was used to calculate the Sc^{44m}/Sc^{44} ratios produced by the reactions K^{41}(10-Mev α,n)Sc^{44} and $Sc^{45}(\alpha,\alpha n)Sc^{44}$ and Sc^{45}(p,pn)Sc^{44} at energies 0.4 Mev above threshold. Agreement between the experimental and calculated Sc^{44m}/Sc^{44} ratio was obtained for the K^{41}(10-Mev α,n)Sc^{44} reaction.

A classical knock-on model was used to calculate the Sc^{44m}/Sc^{44} ratio from a $Sc^{45}(\alpha,\alpha n)Sc^{44}$ or Sc^{45}(p,pn)Sc^{44} reaction in which the charged particle strikes a neutron and both particles go out. This calculated isomer ratio agreed fairly well with the experimental isomer ratio for 320-Mev helium ions which are assumed to have such a small wave length that the projectile interacts classically with only one nucleon.

It is assumed that the K^{41}(43-Mev α,n)Sc^{44} and the $Sc^{45}(\alpha,\alpha n)$ Sc^{44} reactions in the 20- to 43-Mev energy range occur by means of a direct interaction mechanism.

INDEPENDENT YIELDS OF ISOMERIC PAIRS IN NUCLEAR REACTIONS

Sylvia Mae Bailey

Lawrence Radiation Laboratory and Department of Chemistry
University of California, Berkeley, California

April 1959

I. INTRODUCTION

Nuclear isomers are different energy states of the same isotope. The upper member of the isomeric pair differs from an ordinary excited state only in that its half life is measurable. These isomeric pairs usually owe their existence to the large difference in angular momentum between the two states, for the isomeric transition between them is greatly slowed down by the large angular-momentum difference. In the Mayer Shell Model of the nucleus, isomers occur near the end of a nuclear shell where there are small energy differences and large angular-momentum differences between states.

Since isomers are different states of the same isotope, different nuclear reaction and fission mechanisms might be expected to give different yield ratios of the isomeric states. Thus, the study of variations in isomer ratios with varying reaction conditions might give an indication of the reaction mechanisms.

The study of isomer ratios is an interesting problem in its own right, for there is no coherent picutre of the mechanism of isomer formation.

A. Isomer Ratios from Nuclear Reactions

Some of the results in the literature on isomer ratios from nuclear reactions will be reviewed. A literature survey on isomer yields from reactions with thermal neutrons is given by Fairhall,[1] and Segrè[2] tabulated data on isomers from thermal-neutron reactions from the work of Seren.[3] Since a thermal neutron has little energy, the angular momentum, ℓ, of the neutron-target system is zero in thermal-neutron capture. As the neutron spin is 1/2, the compound nucleus has a spin differing from the target nucleus by 1/2. The compound nucleus,

which has the excitation energy of the neutron binding energy, decays by gamma-ray emission in many short steps of $\ell = 1$ or 2 to the isomer products. Excited states in the compound nucleus are expected to decay mainly to the isomer with the nearest spin; that is, states of high angular momentum decay to states of high angular momentum and states of low angular momentum decay to states of low angular momentum. Supportive evidence for this method of gamma decay in the compound nucleus is found from the data on isomer ratios from thermal-neutron reactions. With few exceptions, the isomer ratio is determined by the spins of the target and product nuclei, so that high and low angular-momentum states in the compound nucleus gamma-cascade to isomers of high and low spins respectively. When the compound nucleus has a spin of 1/2 and goes to isomers of spin 1/2 or 3/2 and of spin 9/2 or 11/2, the low-spin isomer has roughly ten times the cross section of the high-spin isomer.

Katz, Pease, and Moody[4] measured the cross sections for the production of Br^{80} isomers by a (γ,n) reaction in the energy range between 11 and 25 Mev. Katz also included a literature survey on the production of Br^{80} isomers by nuclear reactions with projectile energies below 14 Mev. Katz used a compound-nucleus model to calculate the isomer ratio. The spins of the excited compound nucleus are determined by the spins of the interacting particles and the angular momenta ℓ carried by the incoming and outgoing particles. The value of ℓ for neutrons as a function of energy is given by the following formula, which gives the cross section for the formation of the compound nucleus:

$$\sigma_c^{\ell}(E) = \sum (2\ell + 1)\, \pi \lambda^2 \, T_{\ell}(E),$$

where λ is the de Broglie wave length of the incident neutron and $T_{\ell}(E)$ is the transmission coefficient of the nuclear surface for the neutrons. Katz[4] obtained the $T_{\ell}(E)$ values from the graphs of Feld, Feshbach, Goldberger, Goldstein, and Weisskopf.[5] Katz obtained the average ℓ value for the projectile and added this average ℓ value vectorially to the spins of the target and of the projectile to give the spins of the compound nucleus. The spins of the compound nucleus were formed in

proportion to their statistical weight, $2I + 1$. An estimate of the energy and ℓ value of the emitted particle was made in order to obtain the spins of the residual nuclei. The angular-momentum states of the residual nucleus gamma-cascaded to the isomer products with spin values similar to the spin values of the residual nucleus. Katz assumed that the photon reactions occurred by electric dipole absorption. Katz obtained agreement between the calculated and experimentally measured isomer ratios.

Katz and co-workers also reported two other studies[6,7] on isomer yields by (γ,n) reactions in a similar energy range. Sagane[8] obtained a constant yield ratio for the isomers of Mo^{91} produced by a (γ,n) reaction over the energy range from 15 to 67 Mev. This constant isomer ratio was explained in the following way.[6] Only those high-energy (γ,n) reactions which leave the residual nucleus of Mo^{91} below the threshold for further particle emission contribute to the measured Mo^{91} isomers. Even for high-energy photon irradiation, the isomer production comes from photon cascading in a region not too far above threshold.

Fairhall[1] gives some data on isomer ratios for nuclear reactions below 16 Mev.

For the (p,n) reaction at 6.7 Mev, Boehm, Marmier, and Preiswerk[9] measured the yield ratio of the metastable state to the ground state for about fourteen isomer pairs.

All the cases so far discussed gave no clear-cut picture of what would happen if the energy were increased beyond the 5 to 20-Mev range. A review of the suggestions by Segrè and Helmholz[2] and Levy[10] will now be made.

In their 1949 review article on nuclear isomerism, E. Segrè and A. C. Helmholz[2] made a prediction about the formation of isomers at high energies. In discussing the different yields of some isomers formed by the (n,γ) reaction at different neutron energies, they said, "If the energy of the neutrons captured is increased so that capture occurs over many levels of all possible angular momenta, one might

expect that the influence of the level in which the capture occurs will be washed out, and in the limiting case only the statistical weights $(2I + 1)$ of the isomeric states themselves should determine the formation cross section." In the cases discussed, the neutron energies were too low to test their idea. Their reasoning can be extended to other nuclear reactions. The limiting ratio for the isomer formation would be

$$\frac{\sigma_m}{\sigma_g} = \frac{2I_m + 1}{2I_g + 1} ,$$

where σ_m and I_m are the cross section and the spin for the metastable state and σ_g and I_g are the corresponding terms for the ground state. If the ratio σ_m/σ_g were plotted versus energy of the reaction producing the isomers, the curve would approach $(2I_m + 1)/(2I_g + 1)$ asymptotically. This limit could be approached from above or below but would never be crossed.

Levy[10] tested this hypothesis by measuring the isomer ratio for the reaction Mn^{55} (α,n) Co^{58}. Hollander, Perlman, and Seaborg[11] list the spin of Co^{58m} as 5 and the spin of Co^{58} as 2. Strominger, Hollander, and Seaborg[12] list the spin of Co^{58} as 2 and give no spin assignment for Co^{58m}. If the spin of Co^{58m} is 5 and the spin of Co^{58} is 2, the ratio $(2I_m + 1)/(2I_g + 1)$ is 2.2. The isomer ratio did cross the limiting value of 2.2 at about 20 Mev and rose rapidly thereafter. Levy[10] explained this behavior by breaking down the reaction X(a,b)Y into three steps:

1. Formation of the compound nucleus, C^*: $X + a \rightarrow C^*$.
2. Break-up of the compound nucleus to give the excited residual nucleus, Y^*: $C^* \rightarrow b + Y^*$.
3. De-excitation of the excited residual nucleus by successive gamma-ray emission ending in either of the isomeric states:
   $Y^* \rightarrow Y^m + \gamma$, or
   $Y^* \rightarrow Y + \gamma$.

The cross section for the formation of the compound nucleus C^* is given by

$$\sigma^{\ell}_{\text{capt.}} = (2\ell + 1)\, \pi \lambda^2\, T_{\ell}\,(E)\ ,$$

where $T_{\ell}\,(E)$ includes both Coulomb and centrifugal penetrability and goes to 1 as the energy is increased. This favors the capture of particles with high orbital angular momentum. Since $\vec{J} = \vec{\ell} + \vec{I}_x + \vec{I}_a$, the compound nucleus has a wide range of $\vec{J}$ values, with high values preferred by the statistical weight $(2J + 1)$. In the decay of C^*, the spin of the residual nucleus Y^* is determined by $\vec{I}_{Y^*} = \vec{\ell}' + \vec{J} + \vec{I}_b$; therefore, this gives a wide range of spin values, with high spins favored by the statistical weight $(2I_{Y^*} + 1)$. Since in gamma-ray emission the multipole orders may be expected to be dipole or quadrupole, high-spin states of Y^* should decay mainly to the high-spin isomer, and low-spin states of Y^* should decay mainly to the low-spin isomer. Since in each step the formation of the high-spin isomer is favored, there would be no particular limiting value that the ratio σ_m/σ_g would approach at high energies.

Nuclear reactions at low energies, $\leq$ 30 Mev, are usually considered to proceed by the capture of the incident particle to form a compound nucleus in an excited state which then evaporates nucleons. With this compound-nucleus model, one would expect the cross section for a reaction involving a small number of particles out to rise rapidly from threshold but, as higher-order competing reactions become possible, to peak and then to fall rapidly. When observed cross sections do not fall to near zero at energies above that leading to a maximum, but drop to a nonnegligible value, a different reaction mechanism must be postulated at these higher energies. In 1947, Serber[13] advanced qualitative suggestions to explain high-energy reactions. He assumed that at low energies the Bohr compound-nucleus model holds but that, as the incident energy in increased, nuclear transparency becomes important. As the wave length of the incident proton becomes comparable to internucleon distances in the nucleus, the incident nucleon interacts with an individual nucleon in the nucleus, and this interaction is followed by a nucleon-cascade process with or without the emission of further fast particles. If

nuclear matter is represented as a degenerate Fermi gas, collisions having small momentum transfers are discouraged; because these collisions tend to lead from an occupied state to another already occupied state. This effect increases both the mean free path of the high-energy particle (~ 100 Mev) and the mean kinetic energy transfer per collision to the struck particle by a factor of about 5/3. For a 100-Mev nucleon, the mean free path is about 4×10^{-13} cm, and the average kinetic energy transfer to the struck particle is about 25 Mev. Since the mean free path is comparable to nuclear radii, what happens will depend on the particular trajectory of the incident particle. If the incident nucleon passes through the nucleus near the edge, it may make a single collision and emerge with the loss of only about 25 Mev of its energy. Since the struck particles have much lower energy and shorter mean free path then the incident one, they can escape from the nucleus without further collisions only if the collision occurs near the edge of the nucleus, with the struck particle heading outwards and emerging with 15- or 20-Mev energy. Otherwise, the struck particles will collide with other nuclear particles, the energy will be distributed over the nucleus, and the subsequent events can be described in terms of the usual evaporation model with the nuclear excitation energy dissipated by successive boiling off of particles of a few Mev each. Because of the wide distribution of excitation energies of the struck nucleus, there is a wide distribution of residual nuclei after the evaporation processes are complete. Since the mean free path of the incident nucleon varies slowly with the energy of the incident particle, the excitation function at high energies would be expected also to vary quite slowly.

Meadows, Diamond, and Sharp[14] explained their results from high-energy reaction by means of a knock-on mechanism, as Serber[13] suggested. They measured the excitation functions and the yield ratios for the isomeric pairs $Br^{80,80m}$, $Co^{58,58m}$, and $Sc^{44,44m}$ formed in (p,pn) reactions. The spins of the target and product nuclei are taken from Strominger, Hollander, and Seaborg[12] and are listed as follows:

Br^{81} (spin 3/2) (p,pn) $Br^{80,80m}$ (spins of 5 and 1);
Co^{59} (7/2) (p,pn) $Co^{58m,58}$ (spin of 2 for ground state);
Sc^{45} (7/2) (p,pn) $Sc^{44m,44}$ (7 or 6 and 3 or 2).

The ratio $(\sigma_m)/(\sigma_g)$ for Br^{80} rises from about 1.1 at 17 Mev to 1.6 at 30 Mev, drops to 1.3 at 70 Mev, and changes slowly to 1.25 at 100 Mev. The ratio $(\sigma_m)/(\sigma_g)$ for Co^{58} drops suddenly just above threshold from about 4 to about 1.5, and remains constant at that value to 100 Mev. The ratio $(\sigma_m)/(\sigma_g)$ for Sc^{44} is about 0.52 at 13 Mev, rises to about 0.55 at 20 Mev, gradually drops to about 0.41 at 60 Mev, and remains constant out to 100 Mev. In no case does this ratio $(\sigma_m)/(\sigma_g)$ approach as a limit the ratio of the statistical weights. Neither do these ratios $(\sigma_m)/(\sigma_g)$ approach values greatly favoring the high-spin state. Meadows, Diamond, and Sharp[15] made some simple calculations to obtain semi-quantitative values of the ratio of isomer yields at 11 and at 20 Mev. Table I shows their calculation and experimental results.

Table I

Ratio of σ_m/σ_g

The two different values for Sc^{44} are for two different spin assignments

Isomer pair	Calculated		Observed	
	11 Mev	20 Mev	11 Mev	20 Mev
Br^{80}	1.0	2.2	1.0	1.3
Co^{58}	3.1	4.0	1.4(large ?)	1.4
Sc^{44}	0.8,1.7	1.2,2.6	0.52	0.55

The threshold for the reactions is at about 11 Mev, and the largest cross sections are obtained at about 20 Mev, which is assumed to be the peak of the compound-nucleus region. Meadows, Diamond, and Sharp[14] consider the absolute ratios of questionable value but indicative of the change in the ratio with energy. The only protons which were considered to be captured to form a compound nucleus had an angular momentum equal to or less than K R (R is the nuclear radius, K is the wave number of the incident proton). The probability of forming a compound nucleus with definite spin and parity values from an initial nucleus with given spin

and parity was then calculated from the number of ways the spin of the initial nucleus and the angular momentum of the proton could add vectorially to give that spin and parity and from its statistical weight, $(2J + 1)$. At 11 Mev it was assumed that only an s-wave neutron and s-wave proton were emitted to form an excited residual nucleus which gamma cascades to the isomer products nearest in spin to the residual nucleus. The calculations at 20 Mev were similar except that it was assumed that first a p-wave and then an s-wave nucleon were emitted.

The calculations of Meadows, Diamond, and Sharp show a marked increase in the isomer ratio with increasing projectile energy. Since the metastable state has a larger spin than the ground state, this change is to be expected because at higher energies projectiles of higher angular momentum will be captured to form compound nuclei of larger spin. Also, at higher energies, nucleons of higher angular momentum can be emitted to form residual nuclei over a wider range of spin with higher spins favored by their greater statistical weights. They explain the failure of the isomer ratios to increase and the constancy of the isomer ratio at high energy by onset of a knock-on reaction mechanism. The contribution of the compound-nucleus mechanism should be greatest at the cross-section maximum, but at 100 Mev the reaction should proceed entirely by a knock-on mechanism. They point out that "the knock-on mechanism can give a (p,pn) reaction in the following two ways: (1) the incoming proton hits a neutron and both go out; (2) the incoming proton hits a nucleon and only one of the two escapes directly, the other being captured to form an excited compound nucleus which then boils off another nucleon to form the final nucleus." In the first case the excitation energy of the residual nucleus would be less than the binding energy of the next nucleon. The maximum spin would then be the sum of the two single-particle spins. Since only a limited range of excitation energy is permitted, the distribution of spin would show little variation with bombarding energy. In the second case, when one nucleon is captured and the other escapes directly, larger amounts of angular momentum are transferred, and the residual nucleus has an excitation energy less than 20

Mev. "Mixtures of these two knock-on mechanisms, then, should give an isomer ratio intermediate between that at threshold and that at the cross-section peak. Furthermore, when they become the predominant mode of isomer production at energies well above that of the cross-section peak, the isomeric ratio should become constant or only a very slowly varying function of energy."

Pappas and Sharp[16] measured the Cd^{115} isomer-yield ratios from the Sn^{118} (d,αp), Sn^{118} (n,α), In^{115} (d,2p), In^{115} (n,p), and Cd^{114} (d,p) reactions.

The reaction mechanism with high-energy projectiles can be divided into the following two parts: the initial cascade in which the projectile knocks out a few nucleons, and the evaporation according to the compound-nucleus model. The initial cascade has been followed out by means of Monte Carlo calculations in which are considered the successive events in the motion of the incoming nucleon and all its collision partners with their collisions in turn. The actual steps in the calculations are chosen randomly, and the process is arbitrarily cut off when a nucleon reaches some low-energy limit. Morrison[17] describes this picture as applied to high-energy reactions.

Rudstam[18] measured the spallation-cross-section ratios σ_m/σ_g for Zn^{69} from proton bombardments of arsenic. The ratio between the cross section of the high-spin (9/2) isomeric state and the low-spin (1/2) ground state is as follows:

Irradiation energy (Mev):	49	103	170
$\frac{\sigma_{Zn^{69m}}}{\sigma_{Zn^{69}}}$:	2.8±0.2	1.30±0.05	0.76±0.03

Using the Serber model, Rudstam assumed that the evaporation process and gamma cascade are unimportant in changing the isomer ratios. He made Monte Carlo cascade calculations with 470 cascades for 170-Mev protons and 100 cascades for 103-Mev protons. He shows a stepwise plot of cross section versus angular-momentum distribution of the residual nuclides in

the irradiation of arsenic with 170-Mev protons. This graph shows the average spin is 3.1. Therefore, both isomers might be formed in roughly the same yield. No explanation is given for the decrease in isomer ratio from 1.3 at 103 Mev to 0.76 at 170 Mev. He suggests that in the irradiation of arsenic with 49-Mev protons Zn^{69} probably is produced only by means of a compound nucleus. The calculations by Meadows, Diamond, and Sharp[15] indicate that this compound nucleus will have a high spin.

B. Isomer Ratios from Fission

Some ideas about the fission process will be reviewed. Bromley[19] presents the viewpoint that neutron evaporation from the compound nucleus precedes fission. However, the calculations by Vandenbosch, Thomas, Vandenbosch, Glass and Seaborg[20] show that most of the fission precedes neutron evaporation for helium-ion-induced fission of U^{233} and U^{235}. Bromley[19] points out that most authors who have studied fission explain their results by means of variants of Serber's qualitative suggestions advanced in 1947.

Bromley describes the Russian investigations of fission by use of photographic plates, which record the entire fission process. For high-energy fission, the fragments are not emitted at 180° but include a smaller angle about the direction of the incident proton. From the measurement of the angle between the fragments, the recoil velocity is computed. This gives the recoil momentum from which the kinetic energy carried off by the cascade nucleons is calculated. An assumption about the number of nucleons emitted in the cascade is used to obtain the excitation energy of the nucleus before the evaporation stage begins. Bromley shows a graph for the excitation energy of the nucleus prior to the evaporation stage for various bombarding energies and different nuclei. This graph showed good agreement between the Russian photoplate data and the Monte Carlo calculations of McManus.

Bromley reports that Shamov[21] obtained a straight-line relationship between the initial excitation energy and the number of charged

particles emitted per fission. For uranium, Shamov finds that a comparison between the number of charged particles evaporated at fission and the results of evaporation calculations such as those of LeCouteur gives the result that the observed emission is just what one would expect in each case if all the available excitation were to be used up in the evaporation processes. These results are strong evidence for occurrence of the fission process only after the nucleus has lost most of its excitation. Supportive evidence for this picture is the fact that the total kinetic energy of the fission fragments is about the same for thermal neutrons and for high-energy protons.

Bromley gives the following description of high-energy fission. The high-energy particles interact with the target nucleus, leaving it in a highly excited state with high angular momentum. This excitation energy is taken off by multiple-particle emission until the nucleus reaches a low excited state at which particle emission is no longer probable. Theoretical calculations indicate that the evaporated nucleons can carry away relatively large amounts of angular momentum. After the evaporation process, if this low excited state has low angular momentum, then there is a high probability of gamma de-excitation to the ground state and no fission. However, if this low excited state has a high spin, gamma de-excitation is relatively improbable, and the nucleus fissions. Therefore, high-energy fission would actually be a low-excitation phenomenon.

In the work of Vandenbosch, Thomas, Vandenbosch, Glass, and Seaborg,[20] data on cross sections were used to calculate the cross sections for the (α,n), $(\alpha,2n)$, $(\alpha,3n)$, and $(\alpha,4n)$ reactions on U^{233} and U^{235}. The model for these calculations was the Jackson compound-nucleus model. Further calculations showed that most of the fission preceded neutron evaporation in the helium-ion fission of U^{233} and U^{235}. The assumption which is commonly made is that the high fissionability, Z^2/A, of the heavy elements permits fission to precede neutron evaporation but that with less fissionable nuclei neutron evaporation occurs first in order to increase the fissionability of the nucleus.

The experimental data on isomer ratios will be reviewed for both thermal-neutron and high-energy fission. The cumulative yields include both yield from beta-decay chains and independent yield directly from fission. Blomeke[22] lists the yields along decay chains for the products from the thermal-neutron fission of U^{235}. No isomer ratios could be obtained from shielded or independently formed nuclide yields. Steinberg and Glendenin[23] list the cumulative-yield ratios, σ_m/σ_g for Cd^{115} in thermal-neutron fission as follows:

Th^{232}	0.04
U^{238}	0.096
Pu^{239}	0.07
U^{233}	0.005

The ratio of Cd^{115m} (spin 11/2) to Cd^{115} (spin 1/2) from the beta decay of 21-min Ag^{115} is 0.09, and Alexander, Schindewolf, and Coryell[24] report that the 20-sec Ag^{115m} decays in 72% abundance by isomeric transition to Ag^{115} and in 28% abundance by beta decay to the ground state of Cd^{115}. This decay of Ag^{115m} would give an isomer ratio σ_m/σ_g of 0.07. The only isomer ratio, σ_m/σ_g, from thermal-neutron fission which is greatly different from these ratios from the decay of the parent is the 5×10^{-3} ratio from the thermal-neutron fission of U^{233}. This would indicate an independent yield of the low-spin isomer in thermal-neutron fission. However, the evidence for independent isomer yields from thermal-neutron fission is too meager to give an indication whether the high or the low spin is favored.

The experimental data on isomer ratios from high-energy fission will now be reviewed. This review includes the work of Biller,[25] Hicks and Gilbert,[26] and Pappas and Sharp,[16] and a literature search (shown in Table III).

Biller[25] measured several isomer cross sections from 340-Mev proton fission of bismuth. Table II shows the results. The Se^{81} yield, which is from the beta-decay chain, from thermal-neutron fission of U^{235} is included for comparison. In all cases in 340-Mev proton fission of bismuth of spin 9/2, the high-spin isomer was formed in greater yield.

Table II

Isomer yields

Type	Target	Nuclide	Spins		Yields (mb)		Remarks	Spin of target
			Isomer	Ground	Isomer	Ground		
Thermal neutrons	U^{235}	Se^{81}	7/2	1/2	0.008	0.125		7/2
340-Mev protons	Bi^{209}	Se^{81}	7/2	1/2	1.7	---		9/2
	Bi	Zn^{69}	9/2	1/2	0.67	---		
	Bi	Br^{80}	5	1	2.3		shielded	
	Bi	Ag^{110}	6	-	1.9	---	shielded	
	Bi	Nb^{95}	1/2	9/2	0.22	9.9	Precursor has 65-day half life	

The dashes indicate that no corresponding yield of the ground state was detected. Biller's interpretation is that the highly excited states formed immediately after fission are of high spin number.

Hicks and Gilbert[26] measured the ratio of the cross sections for the formation of the Cd^{115m} (spin 11/2) and Cd^{115} (spin 1/2) pair from the high-energy fission of uranium. The cross section of Cd^{115m} was for the independent yield formed directly from fission. Since 28% of Ag^{115m} with half life of 20 sec decays into Cd^{115}, the cross section for Cd^{115} was one of a long-lived end product of a beta-decay chain. The ratio $\sigma\ Cd^{115}/\sigma\ Cd^{115m}$ decreases from 15 for 50-Mev protons to 1.7 for 340-Mev protons. The increased formation of Cd^{115m} at higher energies indicates increasing angular momentum of the fissioning nuclei.

Pappas and Sharp[16] measured the Cd^{115} isomer ratios from 10-Mev to 25-Mev deuteron fission of U^{238}. As with Hicks and Gilbert's work,[26] the independent yield of Cd^{115m} and the cumulative yield of Cd^{115} were determined. When Pappas and Sharp's data are compared with Hicks and Gilbert's data for the 50-Mev to 190-Mev deuteron fission of U^{238}, it is seen that a sharp minimum in the ratio Cd^{115m}/Cd^{115} occurs in the 25-Mev to 50-Mev region.

The results of a literature search on high-energy fission are shown in Table III, which shows the cumulative-yield ratios, Cd^{115m}/Cd^{115}, from fission under a variety of bombarding conditions. The Cd^{115m}/Cd^{115} ratio from the decay of the Ag^{115} parent is 0.09, and 28% of the 20-sec Ag^{115m} decays into the Cd^{115} ground state. For bombarding-particle energies below 45 Mev, the cumulative-yield Cd^{115m}/Cd^{115} ratio from fission is fairly close to 0.09, with the highest value for σ_m/σ_g of 0.228. For bombarding-particle energies above 190 Mev, the cumulative-yield Cd^{115m}/Cd^{115} ratio is much above 0.09, with the lowest value for σ_m/σ_g of 0.34. The increased value of Cd^{115m}/Cd^{115} in high-energy fission must be caused by an increase in the independent yield of Cd^{115m} (high-spin isomer). This increased yield of Cd^{115m} is in agreement with the description by Bromley[19] that high-energy fission is a low-excitation, high-angular-momentum phenomenon. The cumulative-yield Cd^{115m}/Cd^{115} ratio does not vary greatly with projectile energies in the 0.6-Bev to

Table III

Literature search on isomer ratios from fission

Author	Target	Projectile	Projectile energy	Target spin	Isomer pair product	Product spins: Isomer	Product spins: Ground	σ_m/σ_g from fission	Type of yield
Goeckermann and Perlman[27]	Bi	d	190 Mev	9/2	Cd^{115}	11/2	1/2	~1	Cumulative
O'Connor and Seaborg[28]	Natural U	α	380 Mev	0	Cd^{115}			0.5	Cumulative
Folger, Stevenson, and Seaborg[29]	Natural U	p	340 Mev	0	Cd^{115}			0.36	Cumulative
Newton[30]	Th	α	38 Mev	0	Cd^{115}			0.083	Cumulative
Nervik[31]	Ta	p	340 Mev	7/2	Cd^{115}			1.7	Cumulative
Kruger and Sugarman[32]	Th	p	450 Mev	0	Cd^{115}			0.52	Cd^{115} is
	Bi			9/2	Cd^{115m}			1.6	cumulative
	Au			3/2				2.6	Cd^{115m} is
	rhenium			5/2				2.9	independent
	Ta			7/2				2.8	
	holmium			7/2				0.55	
Vinogradov et al.[33]	Natural U	p	480 Mev	0	Cd^{115}			1.1	Cumulative
Wolfgang et al.[34]	Pb	p	0.6 Bev	0,78%	Cd^{115}	11/2	1/2	1.7	Cd^{115} is
			1.0 Bev	1/2,22%	Cd^{115m}			2	cumulative
			1.6 Bev					2.1	Cd^{115m} is
			2.2 Bev					2.5	independent
			3.0 Bev					2.2	
Shudde[35]	Natural U	p	5.7 Bev	0	Cd^{115}	11/2	1/2	0.34	Cumulative
			2.2 Bev					0.45	Cumulative
			0.34 Bev					0.35	Cumulative
Vandenbosch[36]	U^{235}		21.9 Mev	7/2	Cd^{115}	11/2	1/2	0.091	Cumulative
			30.6 Mev					0.10	Cumulative
			42.8 Mev					0.095	Cumulative
			45.5 Mev					0.178	Cumulative
Gibson[37]	Pu^{239}	d	12.3 Mev	1/2	Cd^{115}			0.172	Cumulative
			17.9 Mev					0.224	Cumulative
			23.4 Mev					0.135	Cumulative
	Np^{237}	α	28.1 Mev	5/2		11/2	1/2	0.110	Cumulative
			35.0 Mev					0.228	Cumulative
			45.7 Mev					0.17	Cumulative
	U^{233}	d	12.1 Mev	5/2	Cd^{115}	11/2	1/2	0.184	Cumulative
			19.6 Mev					0.127	Cumulative
			23.4 Mev					0.075	Cumulative
Foreman[38]	Th^{232}	α	27 Mev	0	Cd^{115}			0.066	Cumulative
			36 Mev					0.058	Cumulative
			44 Mev					0.14	Cumulative
Wahl and Bonner[39]	U^{235}	n	14 Mev	7/2	Cd^{115}			0.070	Cumulative
Schmitt and Sugarman[40]	Natural U	photo-fission	16 Mev	0	Cd^{115}	11/2	1/2	0.081	Cumulative
			21 Mev					0.072	Cumulative
			48 Mev					0.087	Cumulative
			100 Mev					0.072	Cumulative
			300 Mev					0.17	Cumulative
Jodra and Sugarman[41]	Bi	p	75-450 Mev	9/2	Nb^{95}	1/2	9/2	1.5	Independent

3.0-Bev proton fission of lead and in the 0.34-Bev to 5.7-Bev proton fission of natural uranium. The work of Vinogradov[33] and that of Kruger and Sugarman[32] show no correlation between the spin of the target nucleus and the Cd^{115m}/Cd^{115} ratio.

Table III shows that the cumulative-yield Cd^{115m}/Cd^{115} ratio in the photofission of natural uranium is close to 0.09, the ratio from the parent Ag^{115}, in the energy range 16 Mev to 100 Mev, but σ_m/σ_g rises to 0.17 at 300 Mev. Sugarman[40] assumes that below 100 Mev the isomers are formed from Ag^{115} and at 300 Mev are beginning to be formed directly from fission.

There is a great difference between the two experimental ratios for Nb^{95m}/Nb^{95} from bismuth fission. The ground state of Nb^{95} has a high spin, and the upper state has a low spin. Biller[35] obtained an independent-yield ratio of 0.022 for Nb^{95m}/Nb^{95}, and Jodra and Sugarman[41] obtained an independent-yield ratio of 1.5 for Nb^{95m}/Nb^{95}. Biller's result agrees with the hypothesis that fission is a high-angular-momentum phenomenon, and Jodra and Sugarman's ratio does not agree with this hypothesis.

In conclusion it may be said that, since there is only one isomer ratio which may be independent from thermal-neutron fission, there is little evidence to support the idea that thermal-neutron fission is a low-angular-momentum phenomenon. In low-energy fission below 45 Mev, a lack of independent isomer ratios prevents the drawing of conclusions about the fission process. In high-energy fission, the work of Biller[25] and of Hicks and Gilbert,[26] and the results in Table III on the Cd^{115m}/Cd^{115} ratio support the suggestion that high-energy fission is a high-angular-momentum phenomenon; however Jodra and Sugarman's Nb^{95m}/Nb^{95} ratio does not support this high-angular-momentum suggestion.

II. EXPERIMENTAL PROCEDURES FOR ISOMERS FROM URANIUM FISSION

A. Target Procedures

Natural uranium foil (about 1 mil and 2 mils thick) was used in bombardments in the 184-inch synchrocyclotron and in the 60-inch cyclotron. Disks, which were punched 1 inch in diameter and cut in half, were clamped in a copper clothespin-type holder and bombarded with 50-Mev to 340-Mev protons in the 184-inch cyclotron. This thin-target arrangement was described by Nervik.[31]

In bombardments on the Crocker Laboratory 60-inch cyclotron, the uranium foil was placed in a "cat's-eye" microtarget assembly like that described by Ritsema[42] except that an oval-shaped instead of a round target was used. Figure 1 shows the microtarget assembly. The target was bombarded with deuterons and helium ions.

B. Chemical Procedures

Cadmium was removed from targets bombarded on the 184-inch cyclotron with protons, and on the 60-inch cyclotron with 12-Mev protons. Promethium was removed from targets bombarded with 45-Mev helium ions on the 60-inch cyclotron. Niobium was removed from targets bombarded with deuterons on the 60-inch cyclotron.

Cadmium

The uranium target foil was dissolved in concentrated nitric acid containing cadmium carrier. The solution was made 4 N in nitric acid, and uranium was extracted with tributylphosphate. The aqueous layer was evaporated almost to dryness, and the residue was dissolved in water. Ferric, lanthanum, and indium carriers were added, the solution was made basic with NH_4OH, and the hydroxides of iron, lanthanum, and indium were centrifuged. Hydrogen sulfide was passed into the solution and the cadmium sulfide precipitate was centrifuged and washed with dilute NH_4OH. Cadmium sulfide was dissolved in 2 N HCl, palladium carrier was added to the solution, H_2S was passed in,

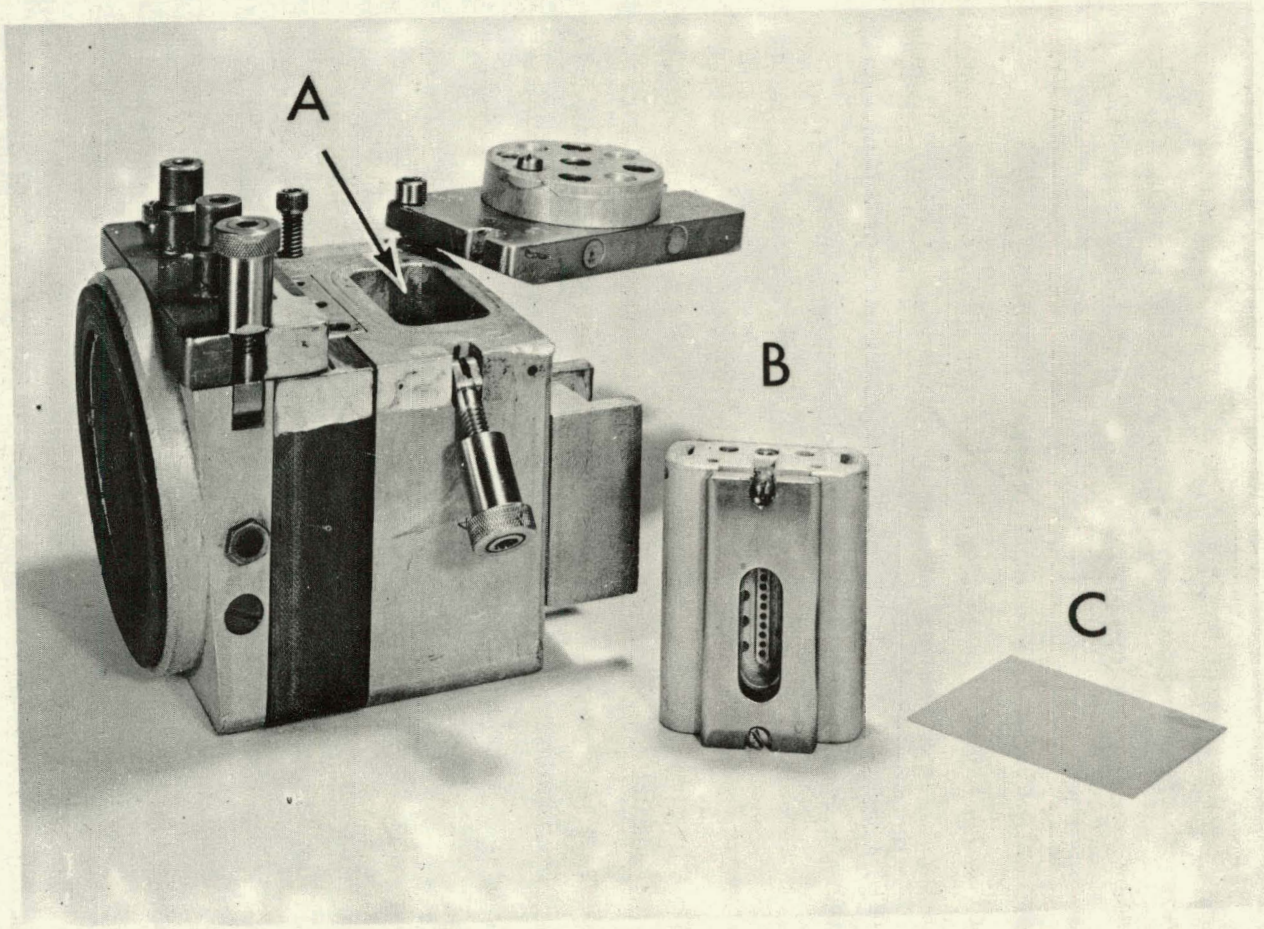

ZN-2123

Fig. 1. Microtarget assembly. A. Microtarget slot, B. Microtarget, C. Degrading foil.

and the palladium sulfide precipitate was centrifuged. Antimony carrier was added, and an Sb_2S_3 scavenge was made. The H_2S was boiled off. Silver carrier was added, and the silver chloride precipitate was centrifuged. Zinc carrier was added, the solution was passed through a 2 mm x 5 cm Dowex A-2 anion-exchange column, and the resin was washed with 0.1 M HCl. Cadmium was eluted with 1.5 N H_2SO_4. This column procedure was suggested by Walter Nervik.[31] H_2S was passed through the eluant; cadmium sulfide was centrifuged, washed with water, ethyl alcohol, and acetone, and dried under a heat lamp. Cadmium sulfide was mounted in an aluminum "hat" for counting as described by Nervik. After the cadmium sulfide was dried in the aluminum dish, which had a depression 1 cm^2 in area, a drop of dilute clear lacquer was placed on the precipitate and dried.

Promethium

The separation of the rare earths from the other fission products was obtained by a chemistry procedure of fluoride and hydroxide precipitations and a Dowex-A-2 resin-column step as described by Nethaway and Hicks.[43] The bombarded uranium foil was placed in a test tube, which contained promethium tracer, yttrium carrier, strontium carrier, and a few drops of hydrogen peroxide. The uranium foil was dissolved by dropping concentrated HCl on it. The solution was diluted to 2 N in hydrochloric acid and made 5 M in hydrofluoric acid. The fluoride precipitate was centrifuged and washed twice with water. The precipitate was dissolved in a mixture of 1 ml of saturated H_3BO_3 and 0.5 ml concentrated nitric acid. The solution was diluted to 10 ml, and one drop of barium holdback carrier was added. The solution was made ammoniacal with NH_3 gas. The hydroxide precipitate was centrifuged and washed twice with dilute NH_4OH. The precipitate was dissolved in 3 ml of concentrated HCl. The solution was passed through a Dowex A-2 resin column 5 mm x 10 cm, and the eluate was collected in a Lusteroid tube. The column was washed with 2 to 3 ml concentrated HCl, and this washing was combined with previous eluate. The solution was diluted to 2 N. Three mg Zr^{+4} and 0.5 ml concentrated H_3PO_4 were added. The precipitate

was centrifuged and discarded. The solution was digested in a hot water bath 2 to 3 minutes with 2 ml 1 M Na_2CrO_4. About five drops of 27 N HF was added. The fluoride precipitate was centrifuged and washed twice with water. The fluoride precipitate was dissolved in 1 ml saturated H_3BO_3 and 0.5 ml concentrated HCl. The solution was diluted to 10 ml and made ammoniacal with NH_3 gas. The hydroxide precipitate was centrifuged and washed twice with water. The precipitate was dissolved in 3 ml concentrated HCl, and the solution was passed through a Dowex A-2 resin column 5 mm x 10 cm long and collected in a tube in which were also collected the 2 to 3 ml concentrated HCl used to wash the column. Then 6 M KOH was added to the eluate until the solution was basic. The hydroxide precipitate was centrifuged and washed twice with water. The precipitate was dissolved in a minimum of concentrated HCl (one or two drops), and the solution was diluted to 4 to 5 ml with water. A few drops of neodymium carrier was added to the solution. About 1 ml Dowex-50 resin was added to the solution, and the mixture was digested in a hot water bath for 10 min with occasional stirring. The resin was then transferred to the top of the resin bed of a Dowex-50 resin column very similar to that described by Nervik.[44]

The Dowex-50 resin column used to separate the rare earths was set up as follows. Dowex-50 cation-exchange resin of "minus 400" mesh size was graded to obtain that portion which settled between 1.0 and 1.5 cm/min in distilled water. The resin was washed with 6 M ammonium thiocyanate until the red ferric thiocyanate color was no longer visible, then washed in turn with distilled water, 6 N hydrochloric acid, and distilled water again. Finally, the resin was converted to the ammonium form with 1 M ammonium lactate and stored in distilled water until loaded on the column. All eluting solutions were 1 M in total lactate concentration and about 0.01 M in phenol to prevent deterioration of the lactate. The dimensions of the ion-exchange resin bed were 7 mm i.d. x 60 cm. This column was surrounded by a water reservoir kept at a temperature of about 90°C by a heating tape. The eluting-agent reservoir system consisted of two 2,000-ml flasks arranged so that, by means of a stopcock control, the solution in the upper flask

could be made to drop into the lower flask at the rate of one drop every 8 to 12 seconds. Both flasks were connected to the laboratory air pressure system through a small air-filtering unit. Before a run, the resin bed was preconditioned by passing through about 100 ml of the eluting agent to be used. The pH of the 1 M lactate eluting agents was adjusted with concentrated ammonium hydroxide and measured on a Beckman Model G pH meter. The pH of the eluting agent in the lower 2,000-ml flask was 3.2, and that in the upper flask was 7.0. Each flask contained about 300 ml initially, and the flow rate between the flasks was about one drop every 8 to 12 sec to give a steadily increasing pH in the eluting agent. Continuous mixing of the solution in the lower flask was assured by a small magnetic stirring device. After a run had begun, samples of the eluent were collected in the collecting tubes over 3-min intervals by means of an automatic sampling turntable. The promethium activity came before the neodymium carrier, which was observed as neodymium oxalate precipitate. For the activity assay, a drop of the eluent from a collecting tube was placed on an aluminum plate and evaporated to dryness under a heat lamp, and the activity was counted in a Geiger-Mueller counter. A peak of promethium activity in the collecting tubes was clearly identified. The solution in the tubes of highest promethium activity was concentrated, placed in a platinum hat, and evaporated to dryness. The platinum hat was mounted for counting.

Niobium

The niobium chemistry was obtained from Hicks.[45] The uranium target foil was dropped into a 40-ml cone containing niobium carrier and 3 drops of hydrogen peroxide. The uranium metal was dissolved by dropping concentrated hydrochloric acid on it and adding H_2O_2. Two milligrams of zirconium carrier was added. Concentrated nitric acid was added, and HCl was boiled off. The solution was digested in a hot water bath. The niobium pentoxide precipitate was centrifuged and washed twice with hot concentrated HNO_3. The Nb_2O_5 precipitate was dissolved in HCl by the following procedure. Ten milliliters of concentrated HCl was added to the precipitate while the Nb_2O_5 was freshly precipitated.

The solution was cooled in an ice bath, saturated with HCl gas, stirred, and digested in a hot water bath. The procedure was repeated (usually twice was sufficient) until the entire precipitate dissolved to give a clear, slightly yellow solution.

The niobium was extracted from 10 M HCl into diisopropyl ketone in a 125-ml Erlenmeyer flask with the use of a mechanical stirrer. Equal volumes of acid and ketone were used.

The niobium was back-extracted from the diisopropyl ketone into 6 M HCl with the use of a mechanical stirrer.

Nb_2O_5 was precipitated with NH_3 gas at a pH of 9. The precipitate was centrifuged, and the solution was discarded. The precipitate was slurried with 5 ml of concentrated HNO_3. The solution was diluted to 20 ml, and the pH was adjusted to 9 with NH_3 gas. The solution was digested. The precipitate was centrifuged and washed twice with hot concentrated HNO_3. The precipitate was transferred to a small crucible, dried under a heat lamp, ignited, and transferred to an aluminum hat for counting.

C. Counting Instruments

The cadmium activity was counted in a Geiger-Mueller counter described by Nervik.[31] The counting unit itself was an end-window, chlorine-argon-filled Amperex type 100 C tube mounted so that samples could be placed on any of five shelves below the end of the tube. This whole assembly was housed inside a 2-inch-thick lead castle to reduce background radiation, and the lead was lined with aluminum to minimize scattering of radiation from the inner walls of the castle. When used in conjunction with a scale-of-256 scaling unit, this counter could handle activities of 80,000 to 100,000 counts per minute without difficulty. At these high counting rates, however, the time between entry of successive beta particles into the sensitive volume of the Geiger-Mueller tube becomes small compared with the resolving time of the counting circuit. In order to get the actual number of particles entering the counter, it is then necessary to correct the observed counting

rate for these coincidence events. The coincidence corrections for the Geiger-Mueller counter had already been determined by workers at the laboratory.

The promethium activity was counted on a Geiger-Mueller counter and on a Nucleometer described by Ritsema.[42] The Nucleometer contains a methane-flow-type windowless proportional counter. The high efficiency of this counter made it particularly useful for following the decay of low-intensity beta-particle emitters.

The niobium activity was counted by following the decay of the 230-kev and 750-kev gamma-ray peaks with a 10-channel gamma-ray pulse-height analyzer. The counting unit in this instrument was a NaI(Tl-activated) scintillation crystal, 1 inch-thick and 1-1/2-inch in diameter, used in conjunction with an RCA 5819 photomultiplier tube. The gamma spectrum was spread over fifty channels which were counted by using the 10-channel analyzer for five consecutive counting periods. Shielding and sample-positioning arrangements for this counter were approximately the same as for the Geiger-Mueller counter. Decay of an individual gamma-ray peak could be followed by counting the sample periodically, plotting the gamma spectra, integrating under the desired peak, and plotting integrated counts as a function of time. The counting efficiency varies with gamma-ray energy.

III. TREATMENT OF DATA

For beta counting the disintegration-rate ratios of samples counted with the same geometry were calculated by dividing the observed counting rate by the following factors: f_a, correction for abundance; f_{eff}, correction for counting efficiency; f_{bks}, backscattering correction; f_{abs}, correction for air and window absorption; f_{SSA}, correction for self-scattering and absorption in the sample. These corrections were described by Nervik.[31]

f_a Correction for Abundance: When a nuclide decays, the radiation that it emits is usually a complex mixture. Its radiation may consist of two or more beta particles of different energies and several gamma rays. When a nuclide with a complicated decay scheme is counted, the abundance of each of the various components of the decay must be known so that each mode of decay may be corrected separately for each of the correction factors. The total "counting efficiency" or conversion factor for a given nuclide may then be obtained by adding the counting efficiencies of the various components of the decay.

f_{eff} Correction for Counting Efficiency: It was assumed that 100% of the beta particles entering the sensitive volume of the Geiger-Mueller tube would be counted. Therefore, $f_{eff} = 1.0$ for beta particles. The counting efficiency of gamma rays in the Geiger-Mueller tube was obtained from the work of Studier and James,[46] and the counting efficiency ranged from 0.5% for 0.25-Mev gamma rays to 1% for 1.0 Mev.

f_{bks} Backscattering Correction Factor: If a weightless sample is placed on a mounting plate which has a macroscopic mass, the observed activity is higher than if there were no mass present. This increase is due to backscattering of beta particles and is a function of the energy of the beta particle and of the thickness and atomic number of the backing material.[47,48] For a given maximum energy of beta particles and a given backing material, f_{bks} increases with increasing backing

thickness until a "saturation" thickness is reached, after which f_{bks} remains constant. For a given beta-particle energy and thick backing materials, the f_{bks} increases with increasing Z of the backscatterer. For a saturation thickness of a given Z and with varying beta-particle energies, f_{bks} increases from 0 to 600 kev and remains approximately constant for all higher-energy beta particles. In order to minimize errors that would be introduced if backscattering corrections were uncertain, the cadmium samples were mounted on aluminum plates thick enough to give saturation backscattering for all beta particles involved. The promethium samples were mounted on platinum thick enough to give saturation backscattering. The backscattering corrections were taken from the data of Burtt.[48]

f_{abs} Correction for Air and Window Absorption: In the "Shelf 1" or "Shelf 2" geometry in which the samples were counted, radiation had to pass through air and mica before entering the sensitive volume of the G-M tube. This thickness of material could easily absorb a significant fraction of beta radiation, especially of low energy. For light elements the absorption thickness in mg/cm^2 is almost independent of the nature of the absorber;[49] therefore, the known mg/cm^2 thickness of mica and air is approximately equivalent to the same thickness of aluminum. Therefore, the correction factor was calculated with the use of the curve of aluminum-absorption half thickness versus beta-ray maximum energy.

f_{SSA} Correction for Self-Scattering and Absorption in the Sample: When any but a weightless sample is counted, the beta radiation emitted may be scattered or absorbed by the mass of the sample itself. The size of this effect depends on the energy of the beta radiation and on the thickness and atomic number of the sample. Nervik and Stevenson[50] have measured f_{SSA} in sodium and lead salts. The self-scattering factor for CdS was measured experimentally by a worker at the laboratory. Since the promethium samples were weightless, the self-scattering factor for the promethium samples was 1.00.

The decay scheme for the cadmium isomers of mass 115 (shown below) was taken from Strominger, Hollander, and Seaborg.[12]

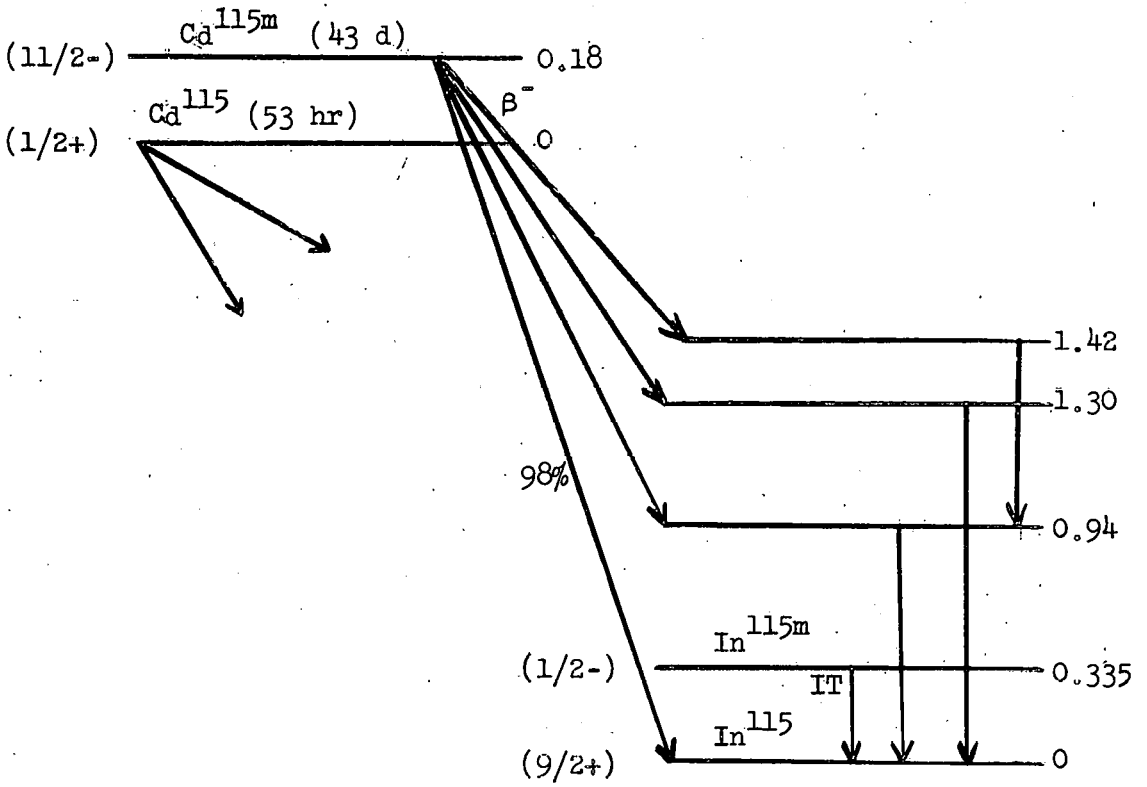

The beta-particle energies and percent abundance for the cadmium and promethium isotopes are taken from Strominger, Hollander, and Seaborg[12] and are as follows:

Isotope	$t_{1/2}$	β^- energy (Mev)
Cd^{115m}	43 d	1.61 (98%); 0.7 (2%)
Cd^{115}	53 hr	0.58 (42%); 1.1 (58%)
Pm^{148}	5.3 d	2.5
Pm^{148}	43 d	2.4 (weak); 0.6
Pm^{149}	54 hr	1.05

The activities of 54-hour Pm^{149} and 43-day Pm^{148} were resolved from the gross G-M-counter decay curve. The 5.3-day Pm^{148} was not present in sufficient quantity to be resolved from the G-M-counter decay curve. By adding arbitrary amounts of 5.3-day Pm^{148} activity to the decay curve, one could see that the cross section for 5.3-day Pm^{148} would have to be at least twice as great as that for 43-day Pm^{148} in order for the 5.3-day Pm^{148} to be visible in the resolution of the decay curve.

The activities of 53-hour Cd^{115} and 43-day Cd^{115m} were resolved from the gross G-M-counter decay curve. The cadmium isomers were further identified by means of gamma spectra and aluminum-absorption curves. The gamma spectra for the cadmium isomers were obtained on a 50-channel gamma-ray pulse-height analyzer. The counting unit in this instrument was a 1-inch thick NaI (Tl-activated) scintillation crystal used in conjunction with an RCA 5819 photomultiplier tube and a 50-channel analyzer.

The decay scheme for the niobium isomers of mass 95, taken from Strominger, Hollander, and Seaborg,[12] is:

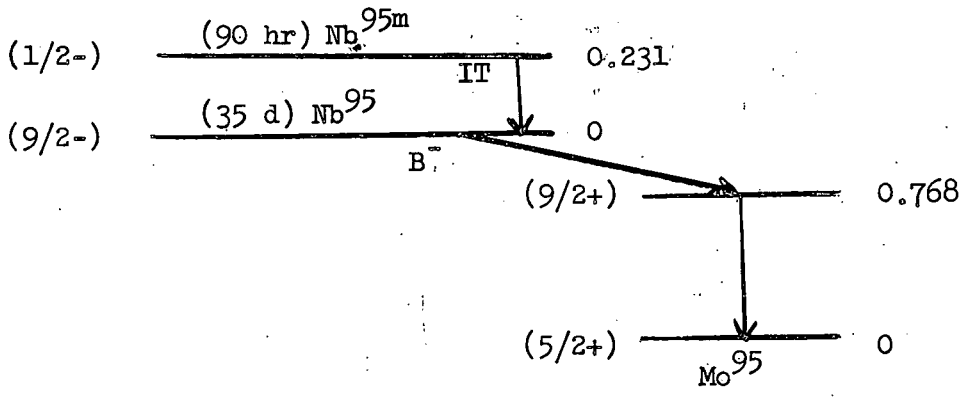

The decays of the 230-kev gamma peak of Nb^{95m} and the 750-kev gamma peak of Nb^{95} were followed. The Compton scattering from the high-energy gamma peak contributed to the counts under the 230-kev peak. After the 230-kev activity had decayed out, the height of the 750-kev peak was normalized to the height of the high-energy peak in the sample that contained the 230-kev peak, and the Compton scattering under the 230-kev

peak was calculated. In this way the 230-kev peak was corrected for the Compton scattering from the high-energy peak. The 750-kev gamma peak decayed with a half life of 35 days. The 230-kev gamma peak decays with a half life of 76 hours, but this half life was uncertain by as much as 15 hours.

The counting efficiency of the sodium iodide (thallium-activated) crystal varies with the energy of the gamma ray. The ratio of the efficiency of the two peaks was obtained from Kalkstein and Hollander.[51]

From the tables of Sliv and Band,[52] the internal-conversion coefficient in the K-shell for the 231-kev gamma ray, which is an M4 transition, was found by interpolation to be 2.60. The internal-conversion coefficients for the 231-kev gamma ray in the L shells were also obtained from the tables of Sliv.[53] The internal-conversion coefficients are 0.352, 0.0580, and 0.106 for the L_I, L_{II}, and L_{III} shells respectively. Thus, the total internal-conversion coefficient for the L shell is 0.516. The total internal-conversion coefficient for shells outside the L shell is assumed to be 40% of the total L-shell conversion coefficient. Therefore, the total internal conversion coefficient for the 231-kev gamma ray is 3.32.

IV. RESULTS ON ISOMERS FROM URANIUM FISSION

As the Pm^{148} isotope is shielded, an attempt was made to determine the independent-yield ratio of 5.3-day Pm^{148} to 43-day Pm^{148} in the 45-Mev helium-ion fission of uranium. However, the presence of a large amount of 54-hour Pm^{149} would make it difficult to see the 5.3-day Pm^{148}. In fact, the experimentally determined ratio of the cumulative yield of Pm^{149} to the independent yeild of 43-day Pm^{148} is 350 ± 100. Although the 5.3-day Pm^{148} was not seen in the decay curves, it is possible to establish an upper limit for the independent-yield ratio of 5.3-day Pm^{148} to 43-day Pm^{148}, which is

$$\frac{Pm^{148}\ (5.3\text{-day})}{Pm^{148}\ (43\text{-day})} < 2 .$$

In the deuteron fission of uranium at 19 to 23 Mev, the independent-yield ratio of Nb^{95m} to the total niobium of mass 95 ranges from 70 to 100%. The accuracy of this ratio depends on the accuracy of the efficiency correction for gamma counting and the accuracy of the conversion coefficients taken from the work of Sliv. Since the upper state, Nb^{95m}, has a low spin and the ground state of Nb^{95} has a high spin, this result is not in agreement with the suggestion that fission is a high-angular-momentum phenomenon.

The cross-section ratios Cd^{115}/Cd^{115m} from the proton fission of natural uranium are shown in Table IV. These ratios are for the cumulative yield. The results in this work are compared with the results of Hicks[26] and Folger[29] for the cumulative-yield ratio.

Table IV

Ratios of cadmium-115 to cadmium-115m

	Proton energy (Mev)					
	350	250	150	90	50	12
Bailey	2.8	3.5	3.8	7.8	18.5	> 31
Hicks	2.3	2.8	4.1	6.7	14	
Folger	2.8					
% agreement of Bailey with Hicks	20%	23%	8%	15%	28%	
Upper limit of Hicks's data	3.3	3.6	5.5	8.6	27	
Lower limit of Hicks's data	2.0	2.1	2.5	3.2	4.9	
% spread in Hicks's data	50%	54%	75%	92%	140%	

V. EXPERIMENTAL PROCEDURES ON Sc^{44} ISOMERS

A. Target Procedures

Spectroscopically pure scandium oxide powder was used as a target for alpha particles on the 60-inch cyclotron and the 184-inch synchrocyclotron. Reagent-grade potassium phosphate tribasic powder was used as a target for alpha particles in the 60-inch cyclotron. About 10 mg of a paste made by mixing Sc_2O_3 powder and Duco cement was spread in a 10-mil platinum "hat." This platinum hat was covered with a 1-mil platinum cover foil and mounted in a microtarget assembly described by Ritsema[42] for bombardment on the 60-inch cyclotron with helium ions. About 15 mg of potassium phosphate K_3PO_4 powder was similarly mounted as a target on the 60-inch cyclotron and bombarded with helium ions. The platinum cover foil was weighed in each bombardment. Weighed aluminum foils were used to degrade the energy of the helium ions from the 60-inch cyclotron as described by Thomas.[54] The energy of the helium ions was obtained from the range-energy curves of Aron, Hoffman, and Williams.[55]

For bombardments on the 184-inch synchrocyclotron with 320-Mev helium ions, a paste of scandium oxide powder and Duco cement was wrapped in aluminum foil about 2 mils thick and clamped in a copper target holder.

B. Chemical Procedures

Scandium was removed from all the targets.

Sc_2O_3 Targets from 60-Inch Cyclotron

The platinum hat containing the scandium oxide was dropped into a centrifuge cone containing about 20 ml of 3 N HCl. About 10 mg of scandium carrier was usually present in the 3 N HCl solution. The solution was heated with occasional stirring for about 1/2 hour in a hot water bath to dissolve the scandium target. The solution was made basic with NH_4OH, and scandium hydroxide was centrifuged and

washed twice with dilute NH_4OH. The scandium hydroxide was dissolved in concentrated HCl, the solution was diluted to 4 N HCl, and 27 N HF was added. After digestion in a hot bath for 1 minute, scandium fluoride was centrifuged and washed twice with water. Scandium fluoride was dissolved in a mixture of 1 ml saturated H_3BO_3 and 0.5 ml concentrated HNO_3 and the solution was diluted to 10 ml. About 0.5 mg calcium holdback carrier was added, the solution was made basic with NH_4OH, and the scandium hydroxide was centrifuged and washed twice with dilute NH_4OH. As described above, another scandium fluoride precipitation and another scandium hydroxide precipitation without adding calcium holdback carrier were made. The scandium hydroxide precipitate was dissolved in concentrated HCl. The solution was diluted to 3 N HCl and passed through a 2 mm x 5 cm Dowex A-2 anion-exchange column. Scandium hydroxide was again precipitated from the solution with NH_4OH and washed with dilute NH_4OH and acetone. For all bombardments below 35 Mev in energy, the scandium hydroxide was mounted in aluminum hats as described in Experimental Procedures for Isomers from Uranium Fission. Scandium hydroxide was mounted in a 1/32-inch lead "hat" with a depression 0.7 cm in diameter and about 0.1 cm deep for all Sc_2O_3 bombardments above 35 Mev in energy. This lead hat was covered with a 1/32-inch lead cover foil and mounted in a 5/16-inch-diameter hole in a 1/2-by-1/16-inch stainless steel strip and held in place by bent flanges. This steel strip was mounted in a definite and fixed position in a Lucite holder for counting.

Sc_2O_3 Targets from 184-Inch Synchrocyclotron

The aluminum foil containing the scandium oxide was dropped into a centrifuge cone. The aluminum foil was dissolved by dropping concentrated HCl on the foil, about 15 ml of 3 N HCl was added, and the solution was heated with occasional stirring for about 1/2 hour in a hot water bath to dissolve the scandium target. A scandium hydroxide and a scandium fluoride precipitation were made as described above. In the next scandium hydroxide precipitation, about 0.5 mg of magnesium

holdback carrier, as well as calcium holdback carrier, was added. The remainder of the chemical procedure was the same as that described for the Sc_2O_3 targets from the 60-inch cyclotron except that the step of passing the 3 N HCl solution through the 2-mm-by-5-cm Dowex A-2 anion-exchange column was omitted.

K_3PO_4 Targets from 60-Inch Cyclotron

The platinum hat containing the potassium phosphate was dropped into a centrifuge cone which contained about 20 mg of scandium carrier. The K_3PO_4 target was dissolved with occasional stirring in about 15 ml of water. The remainder of the chemical procedure was the same as that for Sc_2O_3 targets from the 60-inch cyclotron except that the fluorine precipitations were omitted.

C. Counting Procedures

The scandium activity was counted on a Penco Model PA-3 in which the detecting unit was a sodium iodide (thallium-activated) scintillation crystal. The 1.16-Mev gamma ray of 3.9-hour Sc^{44} and the 270-Mev gamma ray of 59-hour Sc^{44m} were seen.

The decay schemes of Sc^{44m} and Sc^{44}, from Strominger, Hollander, and Seaborg,[12] are:

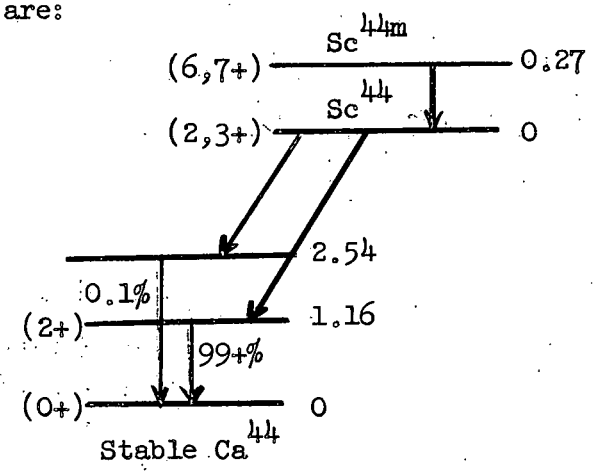

The independent-yield ratio of Sc^{44m} to Sc^{44} was got by following the decay of the 1.16-Mev gamma ray of 3.9-hour Sc^{44}. During the first

day after bombardment, frequent measurements were made of the 1.16-Mev gamma peak, which consisted of the decay of the 3.9-hour Sc^{44} formed by the $(\alpha,\alpha n)$ reaction and of the growth of the 3.9-hour Sc^{44} formed by the isomeric transition of 59-hour Sc^{44m} to Sc^{44}. For several days the decay of the 59-hour Sc^{44m} by isomeric transition to Sc^{44} was followed by counting the 1.16-Mev gamma peak of 3.9-hour Sc^{44} in transient equilibrium with its parent. From the 59-hour decay curve, the growth curve for the 3.9-hour Sc^{44} by isomeric transition was constructed. This Sc^{44} growth curve was subtracted from the experimental decay curve in order to obtain the 3.9-hour decay curve of Sc^{44} formed from the nuclear reaction. From the 3.9-hour decay curve of Sc^{44} and the 59-hour decay curve of Sc^{44} in equilibrium with Sc^{44m}, the independent-yield ratio Sc^{44m}/Sc^{44} was obtained.

The decay of Sc^{44m} is entirely by isomeric transition, with $e/\gamma = 0.14$. The decay of Sc^{44} goes 7% by electron capture and 93% by 1.47-Mev positron. In some bombardments Sc^{43} is formed. The amount of Sc^{43} present is important because 3.9-hour Sc^{43} has a 1.05-Mev gamma ray in 10% abundance. This 1.05-Mev gamma ray will be counted in the 1.16-Mev gamma peak of 3.9-hour Sc^{44} as the half lives of Sc^{43} and Sc^{44} are the same. The decay scheme of Sc^{43}, which is from Strominger, Hollander, and Seaborg,[12] is the following:

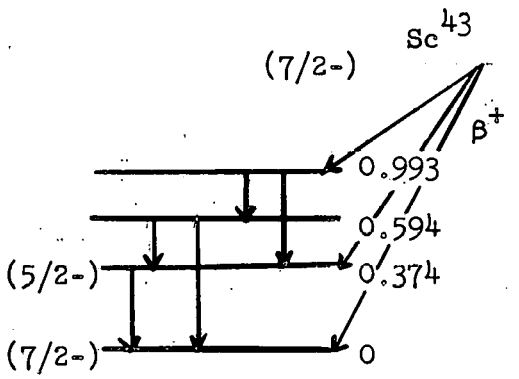

The 3.92-hour Sc^{43} decays 4% by 0.39-Mev β^+, 17% by 0.82-Mev β^+, and 79% by 1.20-Mev β^-. Lindqvist[56] lists the following gamma rays of Sc^{43}:

Energy (Mev)	Relative abundance	Measured in
0.25 ± 0.01	0.5	magn. lens
0.369 ± 0.005	8	magn. lens
0.511	100	magn. lens
0.627 ± 0.005	2	magn. lens
0.84 ± 0.02	weak	scint. spectr.

In Nuclear Level Schemes[57] the following decay scheme for Sc^{43} is listed:

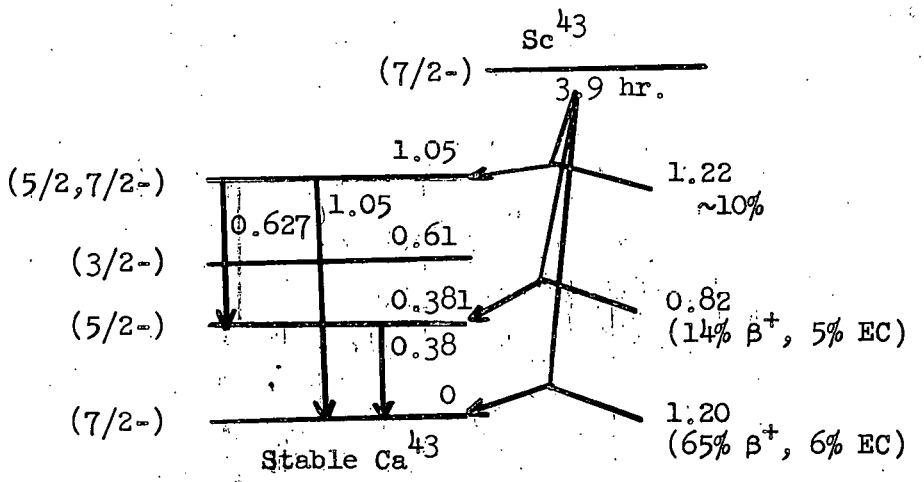

As reported in Nuclear Level Schemes for Sc^{43}, Lieshout and Hayward[58] did not find the 0.627 and 0.84-Mev gamma rays of Sc^{43} but did find a 1.05-Mev gamma ray, which was not in coincidence with the 0.38-Mev β^- and which had the abundance of 10 gamma rays per 100 β^+ events. Therefore, Nuclear Level Schemes lists the gamma rays of Sc^{43} as follows:

Energy (Mev)	Photons/100 β^+
0.25	1
0.369	16
1.05	10

The threshold energies of the reactions $Sc^{45}(\alpha,\alpha n)Sc^{44}$, $Sc^{45}(\alpha,\alpha 2n)Sc^{43}$, $K^{41}(\alpha,n)Sc^{44}$, and $K^{41}(\alpha,2n)Sc^{43}$ were calculated as 12.3, 22.8, 3.65, and 14.3 respectively. The masses for the calculations were taken from Wapstra.[59]

Below a helium-ion energy of 34 Mev the 0.369-Mev gamma ray of Sc^{43} was not seen on the Penco Model PA-3. Below a helium-ion energy of 34 Mev the Sc^{44m}/Sc^{44} ratio was measured by following the decay of the 1.16-Mev gamma-ray peak of Sc^{44} on the Penco Model PA-3 as the 59-hour Sc^{44m} decayed into the 3.9-hour Sc^{44} by isomeric transition. When scandium oxide was bombarded with 43-Mev helium ions, the 370-kev gamma ray of 3.92-hour Sc^{43} was seen on the Penco Model PA-3. Since the 3.92-hour Sc^{43} has the same half life as 3.9-hour Sc^{44}, the 1.05-Mev gamma ray of Sc^{43} cannot be resolved from the decay of the 1.16-Mev gamma-ray peak of Sc^{44}. Since the 1.05-Mev gamma ray of Sc^{43} is not in coincidence with annihilation radiation according to Nuclear Level Schemes, the 1.16-Mev gamma ray of Sc^{44} in coincidence with annihilation radiation was measured by means of a coincidence setup in order to measure the activity of pure Sc^{44}.

The Penco Model PA-3 and a single-channel pulse-height analyzer were used in the coincidence setup. The sodium iodide (thallium-activated) crystals were 1.5-inch in diameter and 1 inch in height. The crystal, photomultiplier tube, and preamplifier were placed in a steel cylinder, which was screwed into a Lucite holder. The angle between these two steel cylinders was 90 degrees. The single-channel pulse-height analyzer was set on the annihilation peak. The variable window width was set at a value that would include the entire annihilation-peak width. The gain position of the center of the annihilation

peak was checked frequently to prevent loss of counts because of drift of the peak position. The counts from the single-channel pulse-height analyzer were used to trigger the gate on the Penco. The gamma rays in coincidence with the annihilation radiation were counted on the Penco.

The gate time was measured by counting two Cs^{137} standards, each shielded from the activity of the other. The activity rate of one Cs^{137} standard was measured by counting on the Penco without coincidence. Then the activity rate of the same Cs^{137} standard with the same geometry was measured on the Penco with the coincidence setup in which the gate was triggered by another Cs^{137} standard with a measured gate rate. From this accidental singles rate, the gate time was calculated by the formula

$$C \times G\tau = C_{chance},$$

with C as Penco count rate without coincidence, G, as gate rate, τ as gate time, and C_{chance} as accidental Penco count rate with coincidence. The gate time was calculated to be 5.71 microseconds. This gate time was used to correct the coincidence counting rate for a 13% accidental singles rate on the 320-Mev helium-ion bombardment of Sc_2O_3. While the 4-hour activity from bombardments was being counted, the length of the gate and the shapes of the signal and gate pulses were monitored with an oscilloscope.

In a Sc_2O_3 target bombarded with 320-Mev helium ions, the 1.16-Mev peak of the 3.9-hour Sc^{44} activity was estimated to contain 3% of the 1.05-Mev peak of 3.9-hour Sc^{43} by calculating from the amount of the 370-kev peak of Sc^{43}. The counting efficiencies for the 0.370- and 1.05-Mev gamma rays were taken from Kalkstein.[51] The Sc^{44m}/Sc^{44} cross-section ratio was 0.61 from counting without coincidence with 4% correction for Sc^{43} and was 0.62 from coincidence counting on another bombardment. When coincidence counting was done on the 4-hour activity, the coincidence counting setup was also used for the 59-hour Sc^{44m} activity in order to avoid making counting corrections.

In the 43-Mev helium-ion bombardments on Sc_2O_3 and on K_3PO_4, the Sc^{44m}/Sc^{44} cross-section ratio was measured by following the 1.16-Mev gamma-ray peak of Sc^{44} by means of the coincidence setup.

In the Sc^{45} (33.7-Mev $\alpha,\alpha n$) Sc^{44} and K^{41} (20.7-Mev α,n) Sc^{44} reactions, the gamma rays were counted with a sodium iodide (thallium-activated) crystal 3 inches in diameter by 3 inches high; in all other bombardments 1.5-by-1-inch crystals were used.

VI. TREATMENT OF DATA ON Sc^{44} ISOMERS

The number of counts in the 1.16-Mev gamma-ray peak of Sc^{44} was computed after background and the Compton scattering from the 1.67-Mev stack-up peak of 0.51- and 1.16-Mev gamma rays were subtracted out.

Forty hours after bombardment, the 1.16-Mev gamma peak of Sc^{44} in transient equilibrium with its parent Sc^{44m} was decaying with the 59-hour half life of Sc^{44m}. When the time required to take the count rate varied from 5% to one-third of the half life, the following formula was used to determine the time $\bar{T}$ for which the measured count rate is the correct rate:

$$\frac{\bar{T} - t}{\Delta t} \cong \frac{1}{2} \left[1 - \frac{5}{6} x + \frac{5}{12} x^2 - \frac{2}{3} x^3 \right]$$

with t as the time when the counting period began, Δt as the length of the counting period, and x as $\lambda \Delta t$. The decay constant λ_1 for Sc^{44m} was taken as 0.0117 $hour^{-1}$, and λ_2 for Sc^{44} as 0.178 $hour^{-1}$ or 0.00297 min^{-1}.

The 59-hour activity of Sc^{44} in transient equilibrium with Sc^{44m} was extrapolated back to the time t_o of the middle of the bombardment. This gives the activity A_2^o of the 3.9-hour Sc^{44} in transient equilibrium with the 59-hour Sc^{44m} parent at time t_o if there had been equilibrium at that time. The activity A_1^o of 59-hour Sc^{44m} at time t_o was found from

$$A_1^o = A_2^o \left(1 - \frac{\lambda_1}{\lambda_2}\right) = 0.934 \; A_2^o .$$

The activity A_2 of the 3.9-hour Sc^{44} which has grown in from the 59-hour Sc^{44m} parent was calculated from the formula

$$A_2 = A_1^o \frac{\lambda_2}{(\lambda_2 - \lambda_1)} \left(e^{-\lambda_1 t} - e^{-\lambda_2 t}\right) = A_2^o \left(e^{-\lambda_1 t} - e^{-\lambda_2 t}\right).$$

This activity rate A_2 was subtracted from the total activity rate during a period of several hours after bombardment to give the activity A_2' of 3.9-hour Sc^{44} which resulted directly from the nuclear reaction and not from the decay of the parent, 59-hour Sc^{44m}. The ratio

$$\frac{A_2^o}{{}_oA_2'} \times \frac{59}{3.9} \times \left(1 - \frac{\lambda_1}{\lambda_2}\right) = 14.1 \frac{A_2^o}{{}_oA_2'}$$

equals the Sc^{44m}/Sc^{44} cross-section ratio with ${}_oA_2'$ as A_2' at t_o.

VII. RESULTS ON Sc^{44} ISOMERS

Table V gives the Sc^{44m}/Sc^{44} cross-section ratio when Sc^{45} (spin 7/2) was bombarded with helium ions at 20.4- to 320-Mev energies. The first column of Table V gives the Sc^{44m}/Sc^{44} cross-section ratio. The second column gives the energy of the helium ions in Mev. The third column gives several conditions under which the 1.16-Mev gamma-ray peak was measured. Since two different Penco Model PA-3 machines were used for counting, the first condition of measurement listed in the third column is which of the two Pencos was used. When the count rate on the Penco was high, the percent of the time that the Penco was not counting was read (as percent) on a dead-time meter on the Penco. This dead-time meter reading should not be trusted to better than five units. The counting rate was corrected for dead time. The dead time affects the isomer ratio because the dead-time reading was close to zero during the decay of the 59-hour Sc^{44m} but was high during the decay of the 3.9-hour Sc^{44} formed in the nuclear reaction. The second condition of measurement listed in the third column is the maximum dead-time reading recorded in the counting. Since two sizes of sodium iodide (thallium-activated) crystals were used in counting gamma rays, the third condition listed in the third column is the dimensions of the crystal. In all coincidence counting, only 1.5-inch-diameter by 1-inch-high crystals were used. The fourth condition listed in the third column is the data of the bombardment. When coincidence counting was used, this is listed. When the Sc^{44m}/Sc^{44} cross-section ratio was corrected for 4% Sc^{43} in the 4-hour activity from the $Sc^{45}(\alpha,\alpha 2n)Sc^{43}$ reaction, this is listed in the third column. An additional part of Table V is the summarized listing of the average Sc^{44m}/Sc^{44} ratio versus the average helium-ion energy.

Table VI gives the Sc^{44m}/Sc^{44} cross-section ratio when K^{41} of spin 3/2 was bombarded with helium ions at 10-Mev to 43-Mev energies. The organization of material in Table VI is similar to that in Table V. The sample which gave 0.5 for Sc^{44m}/Sc^{44} at 10 Mev in Table VI was only one-tenth as strong as the sample which gave 0.24 for Sc^{44m}/Sc^{44} at 10 Mev;

Table V

Sc^{44m}/Sc^{44} ratios for $Sc^{45}(\alpha,\alpha n)Sc^{44}$ reaction

Sc^{44m}/Sc^{44}	Alpha energy (Mev)	Condition of measurement
1.8	20.2	Penco No. 1, 2.5% dead time 1.5xl-in. crystal. 8/5/57
1.6	20.7	Penco No. 2, 20% dead time 3x3-in. crystal. 9/30/57
1.4	25.2	Penco No. 1, 24% dead time 1.5xl-in. crystal. 9/3/57
1.2	25.3	Penco No. 1 and No. 2 14% dead time 1.5xl-in. crystal. 9/9/57
1.5	33.7	Penco No. 2, 27% dead time 3x3-in. crystal. 10/14/57
1.6	33.8	Penco No. 2, 11% dead time 3x3-in. crystal. 10/21/57
1.4	43.0	Penco No. 2 with coincidence counting. 11/22/57 Always used 1.5xl-in. crystals with coincidence counting.
0.58	320	Penco No. 1, 0 dead time 1.5xl-in. crystal. 2/28/58 Ratio corrected for 4% Sc^{43} in the 4-hour activity.
0.58	320	Penco No. 1 with coincidence counting. 2/12/58
0.71	320	Penco No. 1 - same sample as above without coincidence counting. 2/12/58 15% dead time. Ratio corrected for 4% Sc^{43} in 4-hour activity.

$Sc^{45}(\alpha,\alpha n)Sc^{44}$ results summarized

Energy	20.4	25.2	33.7	43	320
Sc^{44m}/Sc^{44}	1.7	1.3	1.5^5	1.4	0.62

as a result, the statistics that gave 0.5 for Sc^{44m}/Sc^{44} were much poorer than the statistics that gave 0.24 for Sc^{44m}/Sc^{44}. Since the samples had decayed through 1-1/2 half lives before the first count was taken, the scatter of the points on an activity-versus-time plot gave a larger chance for error for the weaker sample.

Table VI

Sc^{44m}/Sc^{44} ratios for $K^{41}(\alpha,n)Sc^{44}$ reaction

Sc^{44m}/Sc^{44}	Alpha energy (Mev)	Conditions of measurement
0.24	10	Penco No. 1, 5% dead time. 1.5 x 1-inch crystal. 11/11/57
0.5	10	Penco No. 1, 0 dead time. 1.5 x 1-inch crystal. 11/11/57
0.88	43.3	Penco No. 2 with coincidence counting. 12/17/57

$K^{41}(\alpha,n)Sc^{44}$ results summarized

Energy	10	43
Sc^{44m}/Sc^{44}	0.3 ± 0.1	0.9 ± 0.1

VIII. DISCUSSION

The compound-nucleus model is used for calculating the Sc^{44m}/Sc^{44} isomer ratio produced by the following reactions: K^{41} (10-Mev α,n) Sc^{44} and Sc^{45} (α,αn) Sc^{44} and Sc^{45} (p,pn) Sc^{44} at energies 0.4 Mev above threshold.

The following description is a brief summary of the compound-nucleus calculation. From the addition of the spins of the target nucleus and the incoming particle, the spin S_α of the entrance channel is obtained. The angular momentum ℓ_i of the incoming particle combines with the entrance-channel spin S_α to give the spin J_c of the compound nucleus. These steps are followed through in order to obtain the percentages of the different values of J_c. The compound nucleus emits a particle to give a residual nucleus. Addition of the spins of the residual nucleus and of the outgoing particle give the spin S_β of the exit channel. The angular momentum ℓ_f of the outgoing particle combines with the exit-channel spin S_β to equal the spin of the compound nucleus, J_c. Thus, the exit-channel spin S_β is calculated. From S_β the spin I_2 of the residual nucleus is calculated. These steps are followed through in order to obtain the percentages of the different values of I_2. The residual nucleus drops through a gamma-ray cascade to either of the final products, Sc^{44m}(I = 7 or 6) or Sc^{44} (I = 3 or 2). Thus, the yield ratio of Sc^{44m} to Sc^{44} is obtained.

A. Compound-Nucleus Calculations

Blue and Bleuler[60] gave the following decay scheme for Sc^{44m} and Sc^{44}:

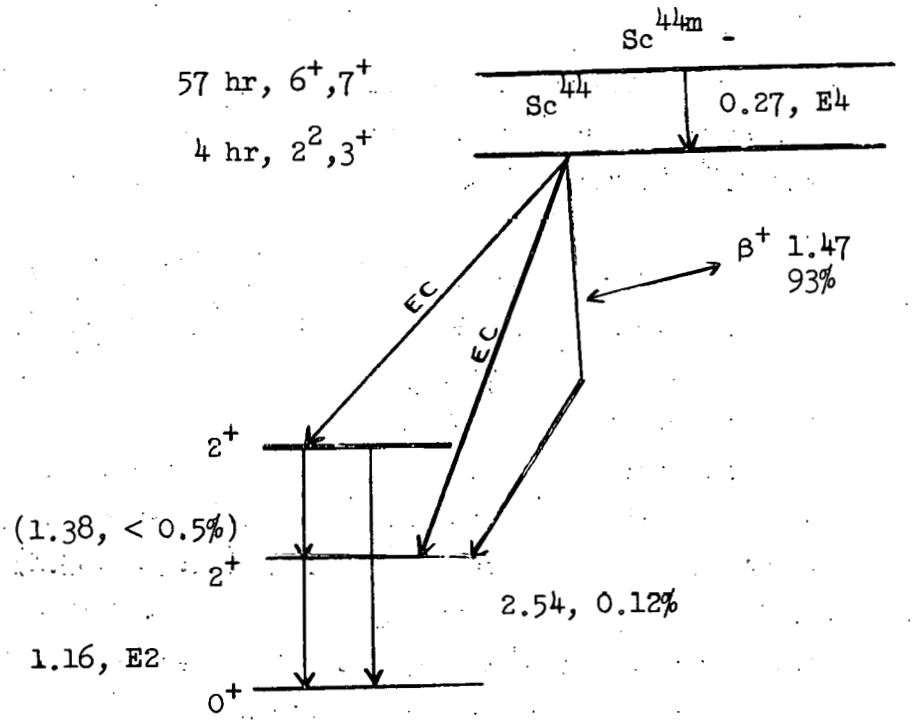

From this decay scheme, it is assumed that Sc^{44m} and Sc^{44} have even parity.

K^{41} (10-Mev α,n) Sc^{44} Calculation

The isomer ratio Sc^{44m}/Sc^{44} from the K^{41} (10-Mev α,n) Sc^{44} reaction was calculated in the following way. The alpha-particle energy of 10 Mev in the laboratory system gives an extrance-channel energy E_α of 9.1 Mev in the center-of-mass system. Since the target nucleus K^{41} has a spin of 3/2+ and the alpha particle has 0 spin, the entrance-channel spin S_α is 3/2+. In the entrance channel, the cross section for the formation of the compound nucleus with a particular angular momentum is given by the formula

$$\sigma_{c_\ell}(\alpha) = (2\ell + 1)\ \pi\ \lambda\!\!\!^{-2}\ T_\ell\ (\alpha),$$

with $\lambda\!\!\!^{-}$ as the de Broglie wave length divided by 2π, $T_\ell(\alpha)$ as the transmission coefficient for each ℓ, and ℓ as the quantum number for the orbital angular momentum according to which the square of the angular momentum equals $\ell(\ell + 1)\ \hbar^2$. The wave number $k = 1/\lambda\!\!\!^{-}$. The trans-

mission coefficient $T_\ell(\alpha)$ was obtained from Feshbach, Shapiro, and Weisskopf.[61] The following constants were calculated for use with the table:

$$\text{Nuclear radius } R = 1.5\, A^{1/3} = 5.17,$$

$$\text{Coulomb barrier } B = 1.442\,\frac{z\,Z}{R} = \frac{1.442 \times 2 \times 19}{5.17} = 10.6 \text{ Mev};$$

$$V_o = \frac{\hbar^2 K}{2M} = \frac{(1.05\times10^{-27})^2 \times (10^{13})^2}{2\times6.65 \times 10^{-24} \times 1.60 \times 10^{-6}} = 5.17 \text{ Mev}$$

with $K = 10^{13}$ cm^{-1} and the alpha-particle mass $M = 6.65 \times 10^{-24}$ g and 1 Mev equals 1.60×10^{-6} erg;

$$V_o/B = 0.49;$$

$g^2 = 0.0694\, z\, Z\, R\, M/M_p = 0.0694 \times 2 \times 19 \times 5.17 \times \frac{6.65}{1.67} = 54.4$ with M_p as proton mass;

$$g = 7.4;$$

$$x = E_\alpha/B = \frac{9.1}{10.6} = 0.86$$

By using $V_o/B = 0.4$, $g = 7$, and $X = 0.9$, one reads off the values of $4/T_\ell$ from the table. The values of T_ℓ for different ℓ are:

ℓ	T_ℓ
0	0.543
1	0.494
2	0.394
3	0.250
4	0.121
5	0.0408
6	0.00983
7	0.00175
8	2.48×10^{-4}
9	2.63×10^{-5}

The results of calculating $\sigma_{c_\ell}(\alpha)$ by the formula

$$\sigma_{c_\ell}(\alpha) = (2\ell + 1)\,\pi\lambda\!\!\!^{-2}\, T_\ell(\alpha)$$

are shown in Table VII.

Table VII

Findings from mathematical calculations for the K^{41} (10-Mev α,n) Sc^{44} reaction

ℓ	$\sigma_{c_\ell}(\alpha)$	% ℓ	J_c
0	0.543	7.30	3/2
1	1.48	19.9	5/2, 3/2, 1/2
2	1.97	26.5	7/2, 5/2, 3/2, 1/2
3	1.75	23.6	9/2, 7/2, 5/2, 3/2
4	1.09	14.7	11/2, 9/2, 7/2, 5/2
5	0.449	6.04	13/2, 11/2, 9/2, 7/2
6	0.128	1.72	15/2, 13/2, 11/2, 9/2
7	0.0262	0.35	17/2, 15/2, 13/2, 11/2
8	0.00421	0.06	19/2, 17/2, 15/2, 13/2
9	0.000500	0.007	21/2, 19/2, 17/2, 15/2

The second column of Table VII gives $\sigma_{c_\ell}(\alpha)$ in units of $\pi \lambda^2$. The third column gives the percent of each ℓ value which contributes inside the nucleus. J_c, the angular momentum of the compound nucleus, is given in the fourth column. The channel spin S_α and ℓ combine to give J_c:

$$J_c = \left| \ell - S_\alpha \right| , \ldots , \ell + S_\alpha .$$

For each S_α and ℓ combination, the percentage of J_c is determined by the statistical weight, $2 J_c + 1$. For example, where ℓ equals 5, the J_c percentages are given as shown below.

J_c	$2 J_c + 1$	% J_c
13/2	14	1.92%
11/2	12	1.65%
9/2	10	1.37%
7/2	8	1.10%

Table VIII shows the calculations of the percentage of J_c formed by alpha particles of various ℓ values.

Table VIII

		Percent of J_c formed by vectorial addition of ℓ values to the entrance-channel spin									
J_c	J_c+1	9	8	7	6	5	4	3	2	1	0
21/2	22	0.002									
19/2	20	0.002	0.02								
17/2	18	0.002	0.02	0.11							
15/2	16	0.001	0.01	0.093	0.53						
13/2	14		0.01	0.082	0.46	1.92					
11/2	12			0.070	0.40	1.65	4.90				
9/2	10				0.33	1.37	4.08	8.44			
7/2	8					1.10	3.26	6.75	10.6		
5/2	6						2.45	5.05	7.95	9.95	
3/2	4							3.37	5.30	6.65	7.30
1/2	2								2.65	3.32	

Table IX shows the percentage of J_c formed by even ℓ in the second column and the percentage of J_c formed by odd ℓ in the third column.

Table IX

Percentage of J_c formed by even and odd ℓ — K^{41} (10 Mev α,n) Sc^{44}

J_c	% J_c from even ℓ	% J_c from odd ℓ
21/2	--	0.002%
19/2	0.02%	0.002%
17/2	0.02%	0.11%
15/2	0.54%	0.094%
13/2	0.47%	2.00%
11/2	5.30%	1.72%
9/2	4.41%	9.81%
7/2	13.9%	7.85%
5/2	10.40%	15.00%
3/2	12.60%	10.01%
1/2	2.65%	3.32%

Cameron[62] compared his formula for nuclear-level spacing with experimental observations up to about $J = 9$ and concluded that, to a good approximation, the nuclear-level spacing was inversely proportional to $(2J + 1)$.

Since the binding energy of an alpha particle in the compound nucleus, Sc^{45}, is 8.0 Mev and E_α is 9.1 Mev, the excitation energy of the compound nucleus is 17.1 Mev. Since the binding energy of a neutron in the compound nucleus Sc^{45} is 11.3 Mev, the maximum kinetic energy available to the emitted neutron is 5.8 Mev. Since the binding energy of a neutron in Sc^{44} is 9.7 Mev, the reaction $K^{41}(\alpha,2n)Sc^{43}$ can not occur.

Donovan, Harvey, and Wade[63] bombarded Bi^{209} with 35-Mev helium ions over an energy range of 7 or 8 Mev. They used a nuclear temperature Θ of 1.4 Mev. Their calculation agreed with the experimental yields when a constant nuclear temperature over several neutron evaporations was assumed in a simple evaporation theory. The reactions studied were $(\alpha,2n)$, $(\alpha,3n)$, and $(\alpha,4n)$. Recoil ranges were measured to check the compound-nucleus model. For the $(\alpha,2n)$ reaction the compound-nucleus model is applicable up to 7 Mev above threshold, for the $(\alpha,3n)$ reaction the compound-nucleus model holds at least to 18 Mev above threshold and perhaps at higher energies, and for the $(\alpha,4n)$ reaction the compound-nucleus model was checked at low energies. Chastel[64] obtained a nuclear temperature Θ of 1.0 Mev for a 10-Mev excitation energy of the residual nucleus in a $Cu(\gamma,p)Ni$ reaction. In the calculations for the $K^{41}(\alpha,n)Sc^{44}$ reaction, the nuclear temperature Θ was assumed to be 1.4 Mev. The average energy of the emitted neutron is twice the nuclear temperature or 2.8 Mev.

Transmission coefficients $T_\ell(\alpha)$ for neutrons are taken from Feld, Feshbach, Goldberger, Goldstein, and Weisskopf.[65] The following constants were calculated for use with the graphs for T_ℓ:

$$R = 1.5\ A^{1/3} = 5.34;$$
$$X_o = K_o R = 5.34 \times 10^{13};$$
$$X = 0.22\ R\ \sqrt{E\ (\text{Mev})} = 0.22 \times 5.34\ \sqrt{2.8} = 1.97.$$

The values of T_ℓ for different ℓ for 2.8-Mev neutrons are:

ℓ	T_ℓ
0	0.775
1	0.700
2	0.455
3	0.130

The formula

$$\sigma_{c_\ell} = (2\ell + 1)\ \pi\ \lambda\!\!\!^{-2}\ T_\ell$$

was used to calculate the cross section for emission of neutrons of different ℓ values.

Table X gives the percentage of different ℓ values of the emitted neutrons in the third column. The second column gives σ_{c_ℓ} in units of $\pi\lambda\!\!\!^{-2}$. The law of conservation of parity, which operates like the

Table X

Percentage of ℓ values of emitted neutrons				
ℓ	σ_{c_ℓ}	% ℓ	% ℓ if ℓ odd	% ℓ if ℓ even
0	0.775	12.8		25.4
1	2.10	34.6	69.8	
2	2.28	37.6		74.6
3	0.910	15.0	30.2	

multiplication of positive and negative signs, is applied to the reaction $K^{41}(\alpha,n)Sc^{44}$. The parity of K^{41} is even, and the intrinsic parities of helium ions, neutrons, and protons are even. Since the shell model of the nucleus shows that states having between twenty and forty particles have odd parity, the assumption is made that for several Mev above the ground state the parity of the odd-odd nucleus Sc^{44} is even. In order to conserve parity, the ℓ values of the neutron must be odd if the ℓ value of the helium ion was odd, and the ℓ value of the neutron must be even if the ℓ value of the helium ion was even. Therefore, in combining the odd ℓ

values of the emitted neutron with J_c formed by an odd ℓ value of the helium ion, the percentages of different ℓ values of the neutron are taken from the fourth column of Table X. Similarly the fifth column of Table X gives the percentages of ℓ for neutrons when the helium ion had even values of ℓ.

The spin states in a nuclear reaction, A(a,c)C, are given as follows:

$$(A + a) \longrightarrow B \longrightarrow (C + c)$$

$$(\vec{I}_1 + \vec{i}_1) + \vec{\ell}_i = \vec{J}_c = \vec{\ell}_f + (\vec{I}_2 + \vec{i}_2)$$

$$\vec{S}_\alpha + \vec{\ell}_i = \vec{J}_c = \vec{\ell}_f + \vec{S}_\beta .$$

Here B is the compound nucleus, ℓ_i and ℓ_f are ℓ values of a and c respectively, I_1 and I_2 are spins of A and B respectively, i_1 and i_2 are intrinsic spins of a and c respectively, S_α is entrance-channel spin, and S_β is exit-channel spin. Table XI shows the combination of ℓ_f, the ℓ value of the emitted neutron, with J_c, the angular momentum of the compound nucleus, to give S_β, the exit-channel spin. The first column of Table XI gives the percent of J_c formed by a helium ion with an even ℓ value, the second column gives the percent of J_c formed by a helium ion with an odd ℓ value, the third column gives J_c, the fourth column gives ℓ_f, the fifth column gives the percent of J_c with this specific combination of ℓ_i and ℓ_f, the sixth column gives the S_β values which result from this combination of ℓ_f and J_c, the seventh column gives the percentages of S_β determined by their statistical weights, $2 S_\beta + 1$.

Table XII gives the total percentages of S_β as they were added up from the preceding table. The exit-channel spin S_β is a combination of the intrinsic neutron spin of 1/2 and the angular momentum of the residual nucleus I_2. The third column gives I_2 from the formula, $I_2 = S_\beta \pm 1/2$. The fourth column gives the percent of I_2 determined by its statistical weight $(2 I_2 + 1)$. The fifth and sixth columns sum up the results of these calculations to give the spins of the residual nucleus at an excitation energy of 3.0 Mev.

Table XI

Methods of the mathematical calculation
K^{41}(10-Mev α,n)Sc^{44} reaction

% J_c if ℓ_i even	% J_c if ℓ_i odd	J_c	ℓ_f	% ℓ combination	S_β	% S_β
	0.002	21/2	1	0.0014	23/2	0.0005
					21/2	0.0005
					19/2	0.0004
			3	0.0006		negligible
0.02	0.002	19/2	1	0.0014	21/2	0.0005
					19/2	0.0005
					17/2	0.0004
			3	0.0006		negligible
			0	0.005	19/2	0.005
			2	0.015	23/2	0.004
					21/2	0.003
					19/2	0.003
					17/2	0.003
					15/2	0.002
0.02	0.11	17/2	0	0.005	17/2	0.005
			2	0.015	21/2	0.004
					19/2	0.003
					17/2	0.003
					15/2	0.003
					13/2	0.002
			1	0.077	19/2	0.029
					17/2	0.026
					15/2	0.023
			3	0.033	23/2	0.0063
					21/2	0.0058
					19/2	0.0052
					17/2	0.0047
					15/2	0.0042
					13/2	0.0037
					11/2	0.0010
0.54	0.094	15/2	0	0.14	15/2	0.14
0.54	0.094	15/2	2	0.40	19/2	0.10
					17/2	0.090
					15/2	0.080
					13/2	0.070
					11/2	0.060
			1	0.066	17/2	0.025
					15/2	0.022
					13/2	0.019

Table XI (cont'd.)

% J_c if ℓ_i even	% J_c if ℓ_i odd	J_c	ℓ_f	% ℓ combination	S_β	% S_β
			3	0.028	21/2	0.0055
					19/2	0.0050
					17/2	0.0045
					15/2	0.0040
					13/2	0.0035
					11/2	0.0030
					9/2	0.0025
0.47	2.00	13/2	0	0.12	13/2	0.12
			2	0.35	17/2	0.090
					15/2	0.080
					13/2	0.070
					11/2	0.060
					9/2	0.050
			1	1.4	15/2	0.53
					13/2	0.47
					11/2	0.40
			3	0.60	19/2	0.12
					17/2	0.11
					15/2	0.10
					13/2	0.086
					11/2	0.074
					9/2	0.061
					7/2	0.049
5.30	1.72	11/2	0	1.35	11/2	1.35
			2	3.96	15/2	1.06
					13/2	0.925
					11/2	0.793
					9/2	0.661
					7/2	0.527
			1	1.20	13/2	0.466
					11/2	0.400
					9/2	0.333
			3	0.520	17/2	0.111
					15/2	0.0990
					13/2	0.0866
					11/2	0.0744
					9/2	0.0619
					7/2	0.0495
					5/2	0.0372
4.41	9.81	9/2	0	1.12	9/2	1.12
			2	3.30	13/2	0.924
					11/2	0.793
					9/2	0.660

Table XI (cont'd.)

% J_c if ℓ_i even	% J_c if ℓ_i odd	J_c	ℓ_f	% ℓ combination	S_β	% S_β
					7/2	0.529
					5/2	0.396
			1	6.85	11/2	2.74
					9/2	2.28
					7/2	1.82
			3	2.96	15/2	0.676
					13/2	0.593
					11/2	0.508
					9/2	0.424
					7/2	0.338
					5/2	0.254
4.41	9.81	9/2	3	2.96	3/2	0.169
13.9	7.85	7/2	0	3.53	7/2	3.53
			2	10.4	11/2	3.12
					9/2	2.60
					7/2	2.08
					5/2	1.56
					3/2	1.04
			1	5.48	9/2	2.28
					7/2	1.83
					5/2	1.37
			3	2.37	13/2	0.593
					11/2	0.508
					9/2	0.424
					7/2	0.338
					5/2	0.254
					3/2	0.170
					1/2	0.085
10.4	15.0	5/2	0	2.64	5/2	2.64
			2	7.76	9/2	2.58
					7/2	2.07
					5/2	1.55
					3/2	1.04
					1/2	0.518
			1	10.5	7/2	4.66
					5/2	3.50
					3/2	2.33
			3	4.53	11/2	1.30
					9/2	1.08
					7/2	0.863
					5/2	0.646
					3/2	0.431

Table XI (cont'd.)

% J_c if ℓ_i even	% J_c if ℓ_i odd	J_c	ℓ_f	% ℓ combinations	S_β	% S_β
10.4	15.0	5/2	3	4.53	1/2	0.216
12.6	10.0	3/2	0	3.20	3/2	3.20
			2	9.41	7/2	3.76
					5/2	2.82
					3/2	1.88
					1/2	0.941
			1	6.98	5/2	3.49
					3/2	2.32
					1/2	1.16
			3	3.02	9/2	1.08
					7/2	0.863
					5/2	0.647
					3/2	0.431
2.65	3.32	1/2	0	0.674	1/2	0.674
			2	1.98	5/2	1.19
					3/2	0.793
			1	2.32	3/2	1.55
					1/2	0.774
			3	1.00	7/2	0.571
					5/2	0.429

Table XII

Derivation of the percent of I_2 values for the K^{41}(10-Mev α,n)Sc^{44} reaction

S_β	% S_β	I_2	% I_2	I_2	% I_2
23/2	0.011	12	0.006	12	0.006
		11	0.005	11	0.015
21/2	0.019	11	0.010	10	0.151
		10	0.009	9	0.379
19/2	0.271	10	0.142	8	1.72
		9	0.129	7	3.69
17/2	0.473	9	0.250	6	8.66
		8	0.223	5	14.23
15/2	2.82	8	1.50	4	20.5
		7	1.32	3	22.6
13/2	4.43	7	2.37	2	18.26
		6	2.06	1	9.03
11/2	12.18	6	6.60	0	1.09
		5	5.59		
9/2	15.70	5	8.64		
		4	7.06		
7/2	23.88	4	13.4		
		3	10.5		
5/2	20.78	3	12.1		
		2	8.66		
3/2	15.35	2	9.60		
		1	5.75		
1/2	4.37	1	3.28		
		0	1.09		

By means of gamma cascades, the residual nucleus goes to the final products, Sc^{44m} (I = 7 or 6) and Sc^{44} (I = 3 or 2). It is assumed that all the I_2 values greater than 7 or 6 decay to 7 or 6 and that all I_2 values less than 3 or 2 decay to 3 or 2. I_2 values within one unit of an isomer spin are assumed to go to that isomer. The spin state midway between the two isomers is divided between the isomers on the basis of their statistical weights.

With the assumption that the spin of Sc^{44m} is 7 and the spin of Sc^{44} is 3, one finds that the ratio of the cross section for the metastable state, σ_m, to the cross section for the ground state, σ_g, is $\sigma_m/\sigma_g = 0.32$. With the assumption that the spin of Sc^{44m} is 6 and the spin of Sc^{44} is 2, one finds that the cross-section ratio is $\sigma_m/\sigma_g = 0.77$. These ratios of σ_m/σ_g are for the K^{41} (10-Mev α,n) Sc^{44} reaction, and the experimental yield ratio, Sc^{44m}/Sc^{44}, for this reaction is 0.3.

$Sc^{45}(\alpha,\alpha n)Sc^{44}$ Calculation

In a similar way a compound-nucleus model was used to calculate σ_m/σ_g for the reaction $Sc^{45}(\alpha,\alpha n)Sc^{44}$ at 0.4 Mev above the threshold. The Q value for the $Sc^{45}(\alpha,\alpha n)Sc^{44}$ and the $Sc^{45}(p,pn)Sc^{44}$ reactions is 11.3 Mev, which is the threshold in the center-of-mass system. In order to make it probable that the two emitted particles will get out of the nucleus, the entrance-channel energy E_α is taken to be 0.4 Mev above the Q value. Therefore, E_α is 11.7 Mev in the calculations on both the reactions, $Sc^{45}(\alpha,\alpha n)Sc^{44}$ and $Sc^{45}(p,pn)Sc^{44}$.

With the use of $V_o/B = 0.5$, g = 8, and X = 1.0, one finds the following transmission coefficients T_ℓ for helium ions from Feshbach, Shapiro, and Weisskopf:[61]

ℓ	T_ℓ	ℓ	T_ℓ
0	0.655	6	0.0506
1	0.623	7	0.0149
2	0.550	8	3.08×10^{-3}
3	0.435	9	5.12×10^{-4}
4	0.285	10	7.05×10^{-5}
5	0.143		

Since the spin of Sc^{45} is 7/2-, the entrance-channel spin S_α is 7/2-.

The formula

$$\sigma_{c_\ell}(\alpha) = (2\ell + 1)\,\pi\lambda^2 T_\ell(\alpha)$$

was used to calculate the cross section for compound-nucleus formation by alpha particles of various ℓ values, and Table XIII shows the results of these calculations. The angular momentum of a compound nucleus is $J_c = \left| \ell - S_\alpha \right|, \cdots, \ell + S_\alpha$

Table XIII

Findings from mathematical calculations for the $Sc^{45}(\alpha,\alpha n)Sc^{44}$ reaction

ℓ	$\sigma_{c_\ell}(\alpha)$	% ℓ	J_c
0	0.655	4.89	7/2
1	1.87	13.9	9/2, 7/2, 5/2
2	2.75	20.5	11/2, 9/2, 7/2, 5/2, 3/2
3	3.05	22.8	13/2, 11/2, 9/2, 7/2, 5/2, 3/2, 1/2
4	2.57	19.2	15/2, 13/2, 11/2, 9/2, 7/2, 5/2, 3/2, 1/2
5	1.57	11.7	17/2, 15/2, 13/2, 11/2, 9/2, 7/2, 5/2, 3/2
6	0.658	4.90	19/2, 17/2, 15/2, 13/2, 11/2, 9/2, 7/2, 5/2
7	0.224	1.67	21/2, 19/2, 17/2, 15/2, 13/2, 11/2, 9/2, 7/2
8	0.0524	0.391	23/2, 21/2, 19/2, 17/2, 15/2, 13/2, 11/2, 9/2
9	0.00975	0.0726	25/2, 23/2, 21/2, 19/2, 17/2, 15/2, 13/2, 11/2
10	0.00148	0.0110	27/2, 25/2, 23/2, 21/2, 19/2, 17/2, 15/2, 13/2

Each S_α and ℓ combination forms J_c values proportional to their statistical weights, $2J_c + 1$. Table XIV shows the percentage J_c formed by alpha particles of both even and odd ℓ values.

Compound nuclei formed just above the energetic threshold with odd parity will be less likely than those with even parity to form $(\alpha,\alpha n)$ and (p,pn) products for the following reasons:

Table XIV

Percentage J_c formed by even and odd ℓ values--$Sc^{45}(\alpha,\alpha n)Sc^{44}$

J_c	even ℓ	odd ℓ
27/2	0.00183	------
25/2	0.00170	0.0124
23/2	0.0706	0.0115
21/2	0.0646	0.317
19/2	1.002	0.288
17/2	0.901	2.66
15/2	5.06	2.36
13/2	4.44	7.77
11/2	9.95	6.67
9/2	8.29	11.33
7/2	11.51	9.07
5/2	4.96	6.72
3/2	3.12	2.16
1/2	0.533	0.815

(a) Since the shell model of the nucleus shows that states having between 20 and 40 particles have odd parity, the assumption is made that for several Mev above the ground state the parity of the odd-odd nucleus Sc^{44} is even.

(b) The assumption is made that the $(\alpha,\alpha n)$ reaction is more likely to occur when only s-wave particles are emitted from the compound nucleus. If these assumptions are made, the parities in the reaction are shown as follows:

$$\underset{\text{odd}}{Sc^{45}} + \underset{\text{odd}}{\alpha} \longrightarrow \underset{\text{even}}{Sc^{44}} + \underbrace{\alpha + n}_{\text{even}}$$

In the calculations, it was assumed that the incoming helium ions which produced the $(\alpha,\alpha n)$ reaction had odd parity.

J_c equals the combination of the sum of the ℓ_f values of the emitted particles and the exit-channel spin S_β; that is,

$$J_c = \left| \ell_f - S_\beta \right|, \cdots \ell_f + S_\beta .$$

Since ℓ_f is zero, the angular momentum of the compound nucleus J_c equals the exit-channel spin S_β. The exit-channel spin S_β is a combination of the spin of the residual nucleus I_2 and the intrinsic spins of the emitted particles; that is, $I_2 = S_\beta \pm 1/2$. Table XV shows the calculations of the spins of the residual nucleus I_2.

With the assumption of I = 7 for Sc^{44m} and I = 3 for Sc^{44}, one finds that the cross-section ratio σ_m/σ_g for isomer formation is σ_m/σ_g = 0.87. With the assumption of I = 6 for Sc^{44m} and I = 2 for Sc^{44}, one finds that σ_m/σ_g is 2.0.

$Sc^{45}(p,pn)Sc^{44}$ Calculation

In a similar way a compound-nucleus model was used to calculate σ_m/σ_g for the $Sc^{45}(p,pn)Sc^{44}$ reaction at 0.4 Mev above the threshold. The constants calculated for use with the tables of Feshbach, Shapiro, and Weisskopf[61] for the transmission coefficients for the incoming proton are: $V_o/B = 3.6$, $g = 3$, and $X = 2.06$. Since the tables give T_ℓ for X values from 0.2 to 1.8, the transmission coefficients T_ℓ for X values of 1.8 were used as shown below:

ℓ	T_ℓ
0	0.800
1	0.765
2	0.660
3	0.457
4	0.195
5	0.0482
6	0.00571
7	0.000635

Table XV

Derivation of the percent of I_2 values for the $Sc^{45}(\alpha,\alpha n)Sc^{44}$ reaction

S_β	% S_β	I_2	% I_2	I_2	Total % I_2
25/2	0.0248	13	0.0129	13	0.0129
		12	0.0119	12	0.0239
23/2	0.0230	12	0.0120	11	0.343
		11	0.0110	10	0.605
21/2	0.634	11	0.332	9	3.08
		10	0.302	8	5.03
19/2	0.576	10	0.303	7	10.55
		9	0.274	6	14.41
17/2	5.32	9	2.81	5	18.6
		8	2.52	4	20.4
15/2	4.72	8	2.51	3	15.79
		7	2.22	2	8.30
13/2	15.54	7	8.33	1	2.84
		6	7.17	0	0.408
11/2	13.34	6	7.24		
		5	6.11		
9/2	22.66	5	12.5		
		4	10.2		
7/2	18.14	4	10.2		
		3	7.94		
5/2	13.44	3	7.85		
		2	5.60		
3/2	4.32	2	2.70		
		1	1.62		
1/2	1.63	1	1.22		
		0	0.408		

The formula

$$\sigma_{c_\ell}(\alpha) = (2\ell + 1)\,\pi\lambda^2\, T_\ell(\alpha)$$

was used to calculate the cross section for compound-nucleus formation by protons of various ℓ values, and Table XVI shows the results of these calculations.

Table XVI

Per cent ℓ values in the formation of the compound nucleus in the $Sc^{45}(p,pn)Sc^{44}$ reaction

ℓ	$\sigma_{c_\ell}(\alpha)$	% ℓ
0	0.800	6.68
1	2.30	19.2
2	3.30	27.6
3	3.20	26.8
4	1.76	14.7
5	0.530	4.43
6	0.0743	0.620
7	0.00953	0.0796

The entrance-channel spins are $S_\alpha = 7/2 \pm 1/2 = 4$ or 3, which are present in proportion to their statistical weights, $2S_\alpha + 1$, therefore the entrance-channel spins of 4 and 3 comprise 56.2% and 43.7% respectively of the entrance channel.

As in the $Sc^{45}(\alpha,\alpha n)Sc^{44}$ reaction, the ℓ value of the incoming proton must be odd in the $Sc^{45}(p,pn)Sc^{44}$ reaction. Table XVII shows the percentages of J_c formed by the different combinations of S_α and ℓ.

From each combination of S_α and ℓ, the percentages of J_c are proportional to their statistical weights, $2J_c + 1$. Since the emitted proton and neutron are s-wave, the angular momentum of the compound nucleus J_c equals the exit-channel spin S_β. The spins of the emitted proton and neutron may add up to 1 or cancel to 0. The calculations for the spin I_2 of the residual nucleus are shown in Table XVIII. From each

Table XVII

Findings from mathematical calculations for the $Sc^{45}(p,pn)Sc^{44}$ reaction

S_α	ℓ	% J_c formed	J_c
4	1	16.6	3, 4, 5
3	1	21.4	2, 3, 4
4	3	29.9	1, 2, 3, 4, 5, 6, 7
3	3	23.2	0, 1, 2, 3, 4, 5, 6
4	5	4.94	1, 2, 3, 4, 5, 6, 7, 8, 9
3	5	3.84	2, 3, 4, 5, 6, 7, 8
4	7	0.0887	3, 4, 5, 6, 7, 8, 9, 10, 11
3	7	0.0690	4, 5, 6, 7, 8, 9, 10

value of S_β, the percentages of I_2 are determined by their statistical weights $2I_2 + 1$. The total percentages of the spin I_2 of the residual nucleus are also given in Table XVIII.

The isomer ratio σ_m/σ_g is calculated as it was for the $Sc^{45}(\alpha,\alpha n)Sc^{44}$ reaction. For Sc^{44m} (I = 7) and Sc^{44} (I = 3), $\sigma_m/\sigma_g = 0.73$, and for Sc^{44m} (I = 6) and Sc^{44} (I = 2), $\sigma_m/\sigma_g = 1.76$.

In bombardments of Bi^{209} with 35-Mev helium ions over an energy range of 7 or 8 Mev, Donovan, Harvey, and Wade[63] found by measuring recoil ranges and angular distributions that the compound-nucleus model holds for energies up to 7 Mev and 18 Mev above threshold for the $(\alpha,2n)$ and $(\alpha,3n)$ reactions respectively. The trend of these figures indicates that an (α,n) reaction would not go by a compound-nucleus mechanism at energies of more than a few Mev above threshold. Therefore, the K^{41} (10-Mev α,n) Sc^{44} reaction, which is 5.8 Mev above threshold, may not proceed by a compound-nucleus mechanism. Consequently, the agreement between the experimental σ_m/σ_g value of 0.3 and the calculated σ_m/σ_g of 0.3 for the K^{41}(10-Mev α,n)Sc^{44} reaction may be accidental. Similarly the Sc^{45}(20-Mev α,n)Sc^{44} reaction, which is 8 Mev above threshold, may not proceed by a compound nucleus mechanism.

Table XIX summarizes the results of the compound-nucleus calculations.

Table XVIII

Derivation of the percent of I_2 values for the $Sc^{45}(p,pn)Sc^{44}$ reaction

S_β	% S_β	I_2	% I_2
11	0.0151	12	0.00547
		11	0.00504
		10	0.00459
10	0.0276	11	0.0101
		10	0.00920
		9	0.00832
9	0.973	10	0.358
		9	0.324
		8	0.290
8	1.718	9	0.640
		8	0.573
		7	0.505
7	8.75	8	3.31
		7	2.92
		6	2.53
6	13.72	7	5.28
		6	4.58
		5	3.87
5	18.37	6	7.24
		5	6.12
		4	5.00
4	24.22	5	9.85
		4	8.06
		3	6.26
3	18.84	4	8.07
		3	6.29
		2	4.49
2	10.37	3	4.84
		2	3.45
		1	2.07
1	2.53	2	1.41
		1	0.843
		0	0.281
0	0.473	1	0.354
		0	0.118

I_2	Total % I_2
12	0.00547
11	0.0151
10	0.372
9	0.972
8	4.17
7	8.71
6	14.35
5	19.84
4	21.13
3	17.39
2	9.35
1	3.27
0	0.399

Table XIX

Results of compound-nucleus calculations

Reaction	Entrance-channel energy	Isomer spins	Calculated σ_m/σ_g	Experimental σ_m/σ_g
$K^{41}(\alpha,n)Sc^{44}$	9.1	7,3 6,2	0.32 0.77	0.3
$Sc^{45}(\alpha,\alpha n)Sc^{44}$	11.7	7,3 6,2	0.87 2.0	---
$Sc^{45}(p,pn)Sc^{44}$	11.7	7,3 6,2	0.73 1.76	0.52

B. Qualitative Remarks

Table XX summarizes the experimental data on the yield ratio of Sc^{44m} to Sc^{44}.

Table XX

Yield ratio Sc^{44m}/Sc^{44} reported by various experimenters

Author	Reaction	Projectile energy (Mev)	Sc^{44m}/Sc^{44}
J. W. Meadows, R. M. Diamond, and R. A. Sharp[14]	$Sc^{45}(p,pn)Sc^{44}$	13	0.52
		20	0.55
		60 to 100	0.41
This work	$Sc^{45}(\alpha,\alpha n)Sc^{44}$	20	1.7
		25 to 43	1.4
		320	0.62
	$K^{41}(\alpha,n)Sc^{44}$	10	0.3
		43	0.9
Boehm[9]	$Ca^{44}(p,n)Sc^{44}$	6.7	0.077
Vinogradov[66]	Proton "fission" of copper	480	0.77

Since Ti^{44}, the parent of Sc^{44}, has a half life of 1000 years,[30] the scandium isomers of mass 44 are effectively shielded; therefore, the measured yields of Sc^{44m} and Sc^{44} from fission are the independent yields, which are formed directly from fission and not from a beta-decay chain.

In the experimental procedures of Meadows, Diamond, and Sharp,[14] any Sc^{43}, which might have been present from an $Sc^{45}(p,p2n)Sc^{43}$ reaction, was counted as Sc^{44}. If an appreciable amount of Sc^{43} was present, the measured Sc^{44m}/Sc^{44} ratio from the (p,pn) reaction would be smaller than it should be. The threshold for the $Sc^{45}(p,p2n)Sc^{43}$ reaction is 21.4 Mev.

It is assumed that the $Sc^{45}(\alpha,\alpha n)Sc^{44}$ reaction in the 20- to 43-Mev energy range does not go by the compound-nucleus mechanism for the following reasons. The Coulomb barrier for the helium ion is about 9.1 Mev, and the binding energy of the neutron in Sc^{45} is 11.3 Mev. Therefore, at a projectile energy of 20 Mev a helium ion and a neutron will not be evaporated from a compound nucleus. Since the experimental isomer ratios are 1.7 at 20 Mev and 1.4 in the 25- to 43-Mev energy range, these similar ratios indicate that the mechanism at 43 Mev is the same as that at 20 Mev. Therefore, these energetic considerations indicate that a compound-nucleus mechanism which evaporates a helium ion does not occur in the 20- to 43-Mev energy range for the $Sc^{45}(\alpha,\alpha n)Sc^{44}$ reaction. Further reactions which could give the Sc^{44} isomers are:

$Sc^{45}(\alpha,2p3n)Sc^{44}$,
$Sc^{45}(\alpha,dp2n)Sc^{44}$,
$Sc^{45}(\alpha,2dn)Sc^{44}$,
$Sc^{45}(\alpha,tpn)Sc^{44}$, and
$Sc^{45}(\alpha,td)Sc^{44}$,

with thresholds of 43, 41, 38, 34, and 32 Mev respectively. The constancy of the experimental isomer ratio in the 25- to 43-Mev energy ranges excludes the contribution of these reactions above their thresholds.

The large yield of the $(\alpha,\alpha n)$ reaction on U^{238} in the 25- to 45-Mev energy range was attributed to a knock-on mechanism and not to a compound-nucleus mechanism by Vandenbosch, Thomas, Vandenbosch, Glass, and Seaborg.[20] They used a compound-nucleus model to calculate the cross sections for the (α,n), $(\alpha,2n)$, $(\alpha,3n)$, and $(\alpha,4n)$ reactions on U^{233} and

U^{235}, and the experimental cross sections measured radiochemically for the $(\alpha,2n)$, $(\alpha,3n)$, and $(\alpha,4n)$ reactions agreed with their calculations. However, the experimental cross sections for the (α,n) reaction did not agree with their calculations. They assumed a direct-interaction mechanism for the (α,n), (α,p), and (α,t) reactions. However, with these fissionable nuclei, the reactions which involve compound-nucleus formation are largely eliminated by fission competition. In a nonfissionable nucleus like Sc^{45}, the prominent compound-nucleus reactions usually mask out any small amounts of direct-interaction reactions.

In bombardments of Bi^{209} with 35-Mev helium ions over an energy range of 7 or 8 Mev, Donovan, Harvey, and Wade[63] found by measuring recoil ranges and angular distributions that the compound-nucleus model holds for energies up to 7 Mev and 18 Mev above threshold for the $(\alpha,2n)$ and $(\alpha,3n)$ reactions respectively. The trend of these figures indicates that a (α,n) reaction would not go by a compound-nucleus mechanism at energies of more than a few Mev above threshold. Therefore, the K^{41}(10-Mev α,n) Sc^{44} reaction, which is 5.8 Mev above threshold, may procede by a knock-on mechanism. At a helium-ion energy of 43 Mev, the $K^{41}(\alpha,n)Sc^{44}$ reaction certainly goes by a knock-on mechanism rather than a compound-nucleus mechanism. Similarly, the Sc^{45}(20-Mev $\alpha,\alpha n)Sc^{44}$, which is 8 Mev above threshold, would not be expected to proceed by a compound-nucleus mechanism. The similarity of the isomer ratios in the 20- to 43-Mev energy range show that the $Sc^{45}(\alpha,\alpha n)Sc^{44}$ reaction at projectile energies of 20 Mev and above proceeds by a knock-on mechanism.

Meadows, Diamond, and Sharp[14] attributed the constancy of the Sc^{44m}/Sc^{44} ratio from the $Sc^{45}(p,pn)Sc^{44}$ reaction at higher energies to the onset of a knock-on mechanism. They obtained a similar constancy in the isomer ratios of Br^{80} and Co^{58} at higher energies, and also explained this constancy by the onset of a knock-on mechanism. Their calculations of the isomer ratio by means of a compound-nucleus model gave rapidly increasing isomer ratios with increasing energy. The results of their calculations for the $Sc^{45}(p,pn)Sc^{44}$ reaction are:

Projectile energy (Mev)	11	11	20	20
Isomer spins	7,3	6,2	7,3	6,2
Calculated σ_m/σ_g	0.8	1.7	1.2	2.6

Since the compound-nucleus calculation gives an isomer ratio of 1.2 at 20 Mev, in disagreement with the experimental ratio of 0.55, it is unlikely that the reaction goes by a compound-nucleus mechanism. A knock-on mechanism is also indicated by the trend of the results of Donovan, Harvey, and Wade.[63] With the possible exception of a projectile energy of just above threshold, the $Sc^{45}(p,pn)Sc^{44}$ reaction goes by a knock-on mechanism. The small difference in the Sc^{44m}/Sc^{44} ratio between 13 Mev, which is just above threshold, and 20 Mev indicates that the $Sc^{45}(p,pn)Sc^{44}$ goes by a knock-on mechanism at all the energies at which the isomer ratio was measured.

The $Sc^{45}(p,pn)Sc^{44}$ and $Sc^{45}(\alpha,\alpha n)Sc^{44}$ reactions can proceed by either of the following two knock-on mechanisms: (a) the charged particle strikes a neutron and both particles go out; (b) the charged particle hits a neutron and only one of the two particles escapes directly; the other particle is captured to form a compound nucleus which boils off another particle to form the final nucleus. Because of the Coulomb barrier for the alpha particle, it is more likely in the latter mechanism that the alpha particle is inelastically scattered and the neutron is boiled off from the compound nucleus. A knock-on calculation for the former mechanism is done below.

C. Knock-on Calculation

This calculation is for a $Sc^{45}(p,pn)Sc^{44}$ or $Sc^{45}(\alpha,\alpha n)Sc^{44}$ reaction in which the charged particle strikes a neutron and both particles go out. This is a classical calculation. In order for the wave length of the projectile to be small enough to enable the projectile to interact classically with only one nucleon, the energy of the projectile must be high. Goldberger[67] assumed that the interaction of 90-Mev neutrons with the nucleus was classical in the sense that the particles had a definite trajectory, because for a 90-Mev neutron the wave length divided by 2π was only 1/18 the nuclear radius.

The binding energy of the least bound particle in the nucleus of Sc^{44} is the 6.87-Mev binding energy of a proton. The Coulomb barrier

for the proton is $V' = 0.7\ V = 0.7 \times 5.60 = 3.92$ Mev.[68] The addition of the proton binding energy and the Coulomb barrier gives a total of 10.8-Mev excitation needed to eject a proton from the Sc^{44} nucleus, but the binding energy of a neutron in Sc^{44} is only 9.86 Mev. Therefore, the energy level of all neutrons knocked out of the nucleus of Sc^{45} in a knock-on reaction must be not lower than 9.86 Mev from the top level in Sc^{44} which has particles in it. The energy-level scheme in the potential well of the nucleus was taken from Ross, Mark, and Lawson.[69] The neutrons in the 1 $f_{7/2}$, 1 $d_{3/2}$, and 2 $s_{1/2}$ levels are certainly available to be knocked out in a knock-on reaction, and the availability of neutrons in the 1 $d_{5/2}$ level is questionable.

A calculation for a knock-on reaction, $Sc^{45}(p,pn)Sc^{44}$ or $Sc^{45}(\alpha,\alpha n)Sc^{44}$, is now made with the assumption that the neutrons in the 1 $f_{7/2}$, 1 $d_{3/2}$, and 2 $s_{1/2}$ levels have equal probabilities of being knocked out. The spin of the knocked-out neutron adds vectorially with the 7/2 spin of the Sc^{45} target to give the spin I_2 of the residual nucleus, which is assumed to gamma-cascade to the isomer products of Sc^{44m} (spin of 7 or 6) and Sc^{44} (spin of 3 or 2). Table XXI shows the combination of neutron and target spins to give the spin I_2 of the residual nucleus.

Table XXI

Vector addition of neutron and target spins to give spin I_2 of residual nucleus

Number of neutrons	Spin of neutron	I_2	Percentage of this combination
4	7/2	7,6,5,4,3,2,1,0	40%
4	3/2	5,4,3,2	40%
2	1/2	4,3	20%

The I_2 spin values are formed in proportion to their statistical weights, $2I_2 + 1$. The percentages of I_2 are shown below:

I_2	% I_2
7	9.38
6	8.13
5	20.7
4	28.2
3	21.9
2	9.37
1	1.87
0	0.63

These spin states gamma-cascade to the isomer nearer in spin, and the I_2 spin midway between the isomer spins goes to both isomers in proportion to their statistical weights. If the spins of Sc^{44m} and Sc^{44} are 7 and 3 respectively, the cross-section ratio of Sc^{44m} to Sc^{44} is 0.46, and, if the spins of Sc^{44m} and Sc^{44} are 6 and 2 respectively, the ratio of Sc^{44m}/Sc^{44} is 1.4.

A similar calculation for the same knock-on reaction is made with the additional assumption that the six neutrons in the 1 $d_{5/2}$ level are also equally available for a knock-on reaction. Table XXII shows the combination of neutron and target spins to give the spin I_2 of the residual nucleus.

Table XXII

Spin I_2 from neutron and target spins			
Number of neutrons	Spin of neutron	Percent of neutrons	I_2
4	7/2	25.0%	7,6,5,4,3,2,1,0
4	3/2	25.0%	5,4,3,2
2	1/2	12.5%	4,3
6	5/2	37.5%	6,5,4,3,2,1

The I_2 spin values are formed in proportion to their statistical weights. The percentages of I_2 are:

I_2	% I_2
7	5.86
6	15.3
5	21.50
4	24.64
3	19.12
2	9.75
1	3.51
0	0.39

These spin states gamma-cascade to the isomer products as in the previous calculation. If the spins of Sc^{44m} and Sc^{44} are 7 and 3 respectively, the cross-section ratio of Sc^{44m} to Sc^{44} is 0.56, and, if the spins of Sc^{44m} and Sc^{44} are 6 and 2 respectively, the ratio of Sc^{44m}/Sc^{44} is 1.5.

The results of these two calculations for the knock-on reactions, $Sc^{45}(\alpha,\alpha n)Sc^{44}$ or $Sc^{45}(p,pn)Sc^{44}$, are summarized below:

Neutron Levels	$1f_{7/2}$, $1d_{3/2}$, $2s_{1/2}$	$1f_{7/2}$, $1d_{3/2}$, $2s_{1/2}$, $1d_{5/2}$
Sc^{44m}/Sc^{44} for spins 7, 3	0.46	0.56
Sc^{44m}/Sc^{44} for spins 6, 2	1.4	1.5

D. Comments on Knock-on Results

Table XXIII shows both calculated and experimental isomer ratios of Sc^{44m}/Sc^{44}.

It is observed that the calculated isomer ratio, 0.46 or 0.56, from the knock-on calculation agrees fairly well with the experimental isomer ratio 0.62 for 320-Mev helium ions. The de Broglie wave lengths,

Table XXIII

Isomer ratios Sc^{44m}/Sc^{44}

Reaction	Projectile energy (Mev)	Isomer spins	σ_m/σ_g calculated	σ_m/σ_g experimental
$Sc^{45}(p,pn)Sc^{44}$	12	7,3	0.73	0.52
		6,2	1.75	
	20	7,3	1.2*	0.55
		6,2	2.6*	
$Sc^{45}(\alpha,\alpha n)Sc^{44}$	20			1.7
	25-43			1.4
	320			0.62
$Sc^{45}(p,pn)Sc^{44}$ or $Sc^{45}(\alpha,\alpha n)Sc^{44}$ by a classical knock-on mechanism in which both particles go out.		7,3	0.46 or 0.56	
		6,2	1.4 or 1.5	

*These ratios were calculated by Meadows, Diamond, and Sharp.[15]

$\lambda = h/\ 2mE$, for various particles are:

λ (fermis)	0.80	2.27	6.37
Particle	320-Mev α	40-Mev α	20-Mev p

Since the de Broglie wave length for 320-Mev helium ions is 0.80×10^{-13} cm or 0.80 fermi, the 320-Mev helium ion is assumed to be small enough for the classical knock-on calculation to be valid. However, since the de Broglie wave lengths for 40-Mev helium ions and 20-Mev protons are 2.27 fermi and 6.37 fermi respectively, these low-energy particles are too large for the classical knock-on calculation to be valid, and a quantum-mechanical calculation for a direct interaction should be made by the method that S. T. Butler[70] used. Such a quantum-mechanical calculation may give an isomer ratio which is different from the classical knock-on calculation. This direct interaction takes place on the surface of the nucleus.

Butler points out such reactions as (n,p), (p,p'), (α,α'), (α,p), etc. have as much chance of proceeding directly as does the deuteron stripping or pickup reaction. In addition to quantum-mechanical calculations for these direct reactions, Butler gives the following semi-classical picture which shows the qualitative features of the angular distributions. When the projectile has a "grazing collision" in the surface shell of radius r_o, the orbital angular momentum ΔL imparted to the initial nucleus through the surface collision is $\Delta L = \ell \hbar$, which equals $\Delta L = \left| \vec{p} \times \vec{r}_o \right|$, with p as the linear momentum imparted to the nucleus. The ℓ value adds vectorially with the spin of the nucleus and the spins of the incoming and outgoing particles to produce the spins of the residual nucleus.

When both particles have the same energy, the helium ion has twice as much angular momentum for the same impact parameter as the proton. Therefore, the isomer ratio from the (α,αn) reaction would be expected to be higher than the isomer ratio from the (p,pn) reaction. In the 20- to 43-Mev energy range, it is observed that the isomer ratio from the (α,αn) reaction is about three times the ratio from the (p,pn) reaction.

It is likely that the $Sc^{45}(p,pn)Sc^{44}$ reaction actually is a $Sc^{45}(p,d)Sc^{44}$ pickup reaction.

E. Summary of Conclusions

From a literature survey on the experimental isomer ratios from fission, the following conclusions are drawn. There is only one isomer ratio which may be independent of thermal-neutron fission. The other isomer ratios from thermal-neutron fission are yields from beta-decay chains. In low-energy fission below 45 Mev, a lack of independent isomer ratios prevents drawing conclusions about the fission process. In high-energy fission, the work of Biller[25] and of Hicks and Gilbert[26] and the results in Table III on the Cd^{115m}/Cd^{115} ratio support the suggestion that high-energy fission is a high-angular-momentum phenomenon; however, Jodra and Sugarman's[41] Nb^{95m}/Nb^{95} ratio does not support this high-angular-momentum suggestion.

Table XXIV summarizes the results of the compound-nucleus calculations.

Table XXIV

Reaction	Entrance-channel energy	Isomer spins	σ_m/σ_g Calculated	σ_m/σ_g Experimental
$K^{41}(\alpha,n)Sc^{44}$	9.1	7, 3 6, 2	0.32 0.77	0.3±0.1
$Sc^{45}(\alpha,\alpha n)Sc^{44}$	11.7	7, 3 6, 2	0.87 2.0	
$Sc^{45}(p,pn)Sc^{44}$	11.7	7, 3 6, 2	0.73 1.75	0.52

The agreement between the experimental $\sigma_m/\sigma_{g_{44}}$ value of 0.3 and the calculated σ_m/σ_g of 0.3 for the K^{41}(10-Mev α,n)Sc^{44} reaction may be accidental because the reaction mechanism may be a knock-on or direct-interaction mechanism instead of a compound-nucleus mechanism. It is assumed that the K^{41}(43-Mev α,n)Sc^{44} reaction procedes by a knock-on mechanism.

It is concluded that, with the possible exception of a projectile energy just above threshold, the $Sc^{45}(p,pn)Sc^{44}$ reaction goes by a knock-on mechanism. It is, however, likely that the $Sc^{45}(p,pn)Sc^{44}$ reaction goes by a knock-on mechanism at all the energies at which the isomer ratio was measured.

It is assumed that the $Sc^{45}(\alpha,\alpha n)Sc^{44}$ reaction in the 20- to 43-Mev energy range goes by a direct-interaction mechanism rather than a compound-nucleus mechanism.

A classical knock-on calculation was made for a $Sc^{45}(p,pn)Sc^{44}$ or $Sc^{45}(\alpha,\alpha n)Sc^{44}$ reaction in which the charged particle strikes a neutron and both particles go out. In this classical calculation, the energy of the projectile must be high enough for the wave length to be small enough to enable the projectile to interact classically with only one nucleon. The results of the classical knock-on calculations are shown below:

Sc^{44m}/Sc^{44} for spins 7 and 3 0.51 ± 0.05

Sc^{44m}/Sc^{44} for spins 6 and 2 1.4^{5}

The Sc^{44m}/Sc^{44} ratio for 7 and 3 spins agrees fairly well with the experimental isomer ratio 0.62 for 320-Mev helium ions, and the de Broglie wave length for the 320-Mev helium ion is assumed to be small enough for the classical knock-on calculation to be valid.

Since the de Broglie wave lengths for 40-Mev helium ions and 20-Mev protons are too large for the classical knock-on calculation to be valid, a quantum-mechanical calculation for a direct interaction should be made by the method that Butler[70] used. Such a quantum-mechanical calculation may give an isomer ratio which is different from the classical knock-on calculation. Butler points out that such reactions as (n,p), (p,p'), (α,α'), (α,p), etc. have as much chance of proceeding directly as does the deuteron stripping or pickup reaction.

When both particles have the same energy, the helium ion has twice as much angular momentum for the same impact parameter as the proton. Therefore, the isomer ratio from the (α,αn) reaction would be expected to be higher than the isomer ratio from the (p,pn) reaction. In the 20- to 43-Mev energy range, it is observed that the isomer ratio 1.5 from the (α,αn) reaction is about three times the ratio 0.5 from the (p,pn) reaction.

It is likely that the Sc^{45}(p,pn)Sc^{44} reaction actually is a Sc^{45}(p,d)Sc^{44} pickup reaction.

ACKNOWLEDGMENTS

I wish to express by gratitude to Professor Isadore Perlman, under whose guidance this work was done.

I wish to thank Richard A. Glass for his helpful discussions and interest.

I wish to thank Frank S. Stephens, Jr., Frank Asaro, Bernard G. Harvey, Professor John O. Rasmussen, Walter E. Nervik, Paul A. Benioff, Susanne Vandenbosch (nee Ritsema), and Richard M. Diamond for their helpful discussions.

I am grateful to George W. Kilian for help in arranging the electronic setup for the gamma-ray coincidence counting.

I wish to thank Roberta B. Garrett and Thérèse K. Pionteki for valuable assistance in the beta-ray counting of samples.

The cooperation of Peter McWalters, W. Bart Jones, the late G. Bernard Rossi, and other members of the crew of the Crocker Laboratory 60-inch cyclotron is appreciated.

The cooperation of Mr. J. T. Vale and Mr. Lloyd Hauser and all those of the 184-inch cyclotron group is gratefully acknowledged.

I wish to thank J. G. Conway, R. D. McLaughlin, and G. V. Shalimoff, who provided spectrographic analyses of materials to indicate their purity.

The cooperation of Almon E. Larsh and Alfred A. Wydler in repairing the Pencos is gratefully acknowledged.

The assistance of the Health Chemistry Group under the direction of Nelson Garden is appreciated, especially that of Jacqueline Forslund, Lewis Potter, Sue Hargis, Roberta Delk, Marshall Lombardo, and Evelyn White.

I am grateful to Charlotte Mauk for editing this manuscript, and to Patricia Howard and Lilly Hirota for the typing of the Multilith originals for this thesis.

This work was performed under the auspices of the U. S. Atomic Energy Commission.

REFERENCES

1. A. W. Fairhall, Massachusetts Institute of Technology, Laboratory for Nuclear Science and Engineering, Progress Report, MIT-NSE-PR (5-31-52), May 31, 1952, p. 131.

2. E. Segrè and A. C. Helmholz, Revs. Modern Phys. 21, 271 (1949).

3. L. Seren, H. N. Friedlander, and S. H. Turker, Phys. Rev. 72, 888 (1947).

4. L. Katz, L. Pease, and H. Moody, Can. J. Phys. 30, 476 (1952).

5. B. T. Feld, H. Feshbach, M. L. Goldberger, H. Goldstein, and V. F. Weisskopf, Final Report of the Fast Neutron Data Project, NYO-636, Jan. 1951.

6. L. Katz, R. G. Baker, and R. Montalbetti, Can. J. Phys. 31, 250 (1953).

7. J. Goldemberg and L. Katz, Phys. Rev., 90, 308 (1953).

8. R. Sagane, Phys. Rev. 85, 926 (1952).

9. F. Boehm, P. Marmier, and P. Preiswerk, Helv. Phys. Acta 25, 599 (1952).

10. Harris B. Levy, I. Isomeric States of Bismuth-210. II. Relative Yields in the Formation of Nuclear Isomers (thesis), UCRL-2305, Aug. 1953.

11. J. M. Hollander, I. Perlman, and G. T. Seaborg, Table of Isotopes, UCRL-1928-Rev., Dec. 1952.

12. D. Strominger, J. M. Hollander, and G. T. Seaborg, Revs. Modern Phys. 30, 585 (1958).

13. R. Serber, Phys. Rev. 72, 1114 (1947).

14. J. W. Meadows, R. M. Diamond, and R. A. Sharp, Phys. Rev. 102, 190 (1956).

15. J. W. Meadows, R. M. Diamond, and R. A. Sharp, Harvard University, Cambridge, Massachusetts, Excitation Functions and Yield Ratios for the Isomeric Pairs $Br^{80,80m}$, $Co^{58,58m}$, and $Sc^{44,44m}$ Formed in (p,pn) Reactions, (unpublished manuscript), 1956.

16. Alexis C. Pappas and Rodman A. Sharp, The Chemical Institute, University of Oslo, Blindern, Norway, Cd^{115} Isomer Yield Ratios from Deuteron Fission of U^{238} and from the $Sn^{118}(d,\alpha p)$, $Sn^{118}(n,\alpha)$, $In^{115}(d,2p)$, $In^{115}(n,p)$, and $Cd^{114}(d,p)$. (Unpublished manuscript to be published in J. Inorg. Nuclear Chem.)

17. Philip Morrison in Experimental Nuclear Physics, E. Segrè, Ed., Vol. II (John Wiley and Sons, New York, 1953), p. 141, Sect. 11.

18. Gösta Rudstam, Spallation of Medium Weight Elements (thesis), NP-6191, University of Uppsala, 1956.

19. D. A. Bromley, in Proceedings of the Symposium on the Physics of Fission held at Chalk River, Ontario, May, 1956, CRP-642-A, July 1956, p. 65.

20. R. Vandenbosch, T. D. Thomas, S. E. Vandenbosch, R. A. Glass, and G. T. Seaborg, Phys. Rev. 111, 1358 (1958).

21. V. P. Shamov, Doklady Akad. Nauk. S.S.S.R. 103, 593 (1955).

22. J. O. Blomeke, Uranium-235 Fission-Product Production as a Function of Thermal Neutron Flux Irradiation Time and Decay Time. I. Atomic Concentrations and Gross Totals. ORNL-2127, Aug. 1957.

23. E. P. Steinberg and L. E. Glendenin, in Proceedings of the International Conference on the Peaceful Uses of Atomic Energy, Geneva, 1955, Vol. 7, p. 3.

24. J. M. Alexander, V. Schindewolf, and Charles D. Coryell, Phys. Rev. 111, 228 (1958).

25. William F. Biller, The Characteristics of Bismuth Fission Induced by 340-Mev Protons (thesis), UCRL-2067, March 1953.

26. Harry G. Hicks and Richard S. Gilbert, Phys. Rev. 100, 1286 (1955).

27. R. H. Goeckermann and I. Perlman, Phys. Rev. 73, 1127 (1948).

28. P. R. O'Connor and G. T. Seaborg, Phys. Rev. 74, 1189 (1948).

29. Folger, Stevenson, and Seaborg, Phys. Rev. 98, 107 (1955).

30. A. S. Newton, Phys. Rev. 75, 17 (1949).

31. Walter E. Nervick, Tantalum Spallation and Fission Induced by 340-Mev Protons (thesis), UCRL-2542, April 1954.

32. P. Kruger and N. Sugarman, Phys. Rev. 99, 1459 (1955).

33. A. P. Vinogradov, I. P. Alimarin, V. I. Baranov, A. K. Lavrukhina, T. V. Baranova, F. I. Pavlotskaya, A. A. Bragina, and Yu. V. Yakovlev, in Meetings of the Division of Chemical Sciences, Session of the Academy of Sciences of the USSR on Peaceful Uses of Atomic Energy, July 1-5, 1955 (Publishing House of the Academy of Sciences of the USSR, Moscow, 1955), pp.65-78.

34. Wolfgang, Baker, Caretto, Cumming, Friedlander, and Hudis, Phys. Rev. 103, 394 (1956).

35. Rex H. Shudde, Fission of Uranium with 5.7-Bev Protons (thesis), UCRL-3419, June 1956.

36. Robert Vandenbosch, Fission and Spallation Competition in Ra^{226}, Th^{230}, U^{235}, and Np^{237} (thesis), UCRL-3858, July 1957.

37. Walter M. Gibson, Fission and Spallation Competition from the Intermediate Nuclei Am^{241} and Np^{235} (thesis), UCRL-3493, Nov. 1956.

38. Bruce M. Foreman, Jr., Spallation and Fission in Thorium-232 and the Masses of the Heaviest Elements (thesis), UCRL-8223, April 1958.

39. Arthur C. Wahl and Norman A. Bonner, Phys. Rev. 85, 570 (1952).

40. R. A. Schmitt and N. Sugarman, Phys. Rev. 95, 1260 (1954).

41. L. G. Jodra and N. Sugarman, Phys. Rev. 99, 1470 (1955).

42. Susanne E. Ritsema, Fission and Spallation Excitation Functions of U^{238} (Master's thesis), UCRL-3266, Jan. 1956.

43. D. R. Nethaway and H. G. Hicks, Radiochemical Procedures in Use at the University of California Radiation Laboratory (Livermore), UCRL-4377, Aug. 1954.

44. Walter E. Nervik, J. Phys. Chem. 59, 690 (1955).

45. Harry Hicks, Anal. Chem. 26, 1205 (1954).

46. M. Studier and R. James (UCRL) Unpublished data, 1946.

47. Conference on Absolute β Counting, National Research Council, NP-1813, Oct. 1950.

48. P. B. Burtt, Nucleonics, page 28 (Aug. 1949).

49. Samuel Glasstone, Sourcebook on Atomic Energy (D. Van Nostrand Co., New York, 1950), p. 165.

50. W. Nervik and P. C. Stevenson, Nucleonics 10, 18 March 1952.

51. M. I. Kalkstein and J. M. Hollander, "A Survey of Counting Efficiencies for a 1-1/2-inch-Diameter by 1-inch-High Sodium Iodide (Thallium Activated) Crystal," UCRL-2764, Oct. 1954.

52. L. A. Sliv and I. M. Band, "Coefficients of Internal Conversion of Gamma Radiation, Part I. K-Shell," Academy of Sciences of the U.S.S.R., Moscow-Leningrad (1956). Issued in U.S.A. as Report 57 ICC KI, Physics Department, University of Illinois, Urbana, Illinois.

53. L. A. Sliv and I. M. Band, "Tables of Internal Conversion Coefficients of Gamma Radiation, Part 2. L-Shell," published by the Academy of Sciences of the U.S.S.R., Moscow-Leningrad (1958).

54. Thomas Darrah Thomas, "Spallation-Fission Competition from the Compound System U^{233} Plus He^{4}" (thesis), UCRL-3791, July 1957.

55. Aron, Hoffman, and Williams, Range-Energy Curves, AECU-663, May 1951.

56. Torsten Lindqvist and Allen C. G. Mitchell, Phys. Rev. 95, 1535 (1954).

57. Nuclear Level Schemes, A = 40 to A = 92, June (1955), Committee on Tables of Constants and Numerical Data, National Academy of Sciences — National Research Council, Washington, D. C.

58. R. van Lieshout and R. W. Hayward, private communication to the editors of Nuclear Level Schemes, March, 1955; $Ca^{(40)}$ (17-Mev α,p).

59. A. H. Wapstra, "Isotopic Masses II $33 < A < 202$," Physica 21, 384-409 (1955).

60. J. W. Blue and E. Bleuler, Phys. Rev. 100, 1324 (1955).

61. Herman Feshbach, M. M. Shapiro, and V. F. Weisskopf, Tables of Penetrabilities for Charged Particle Reaction, NYO-3077; NDA-15B-5, June 1953.

62. A. G. W. Cameron, Nuclear Level Spacings, Chalk River Report, PD-292, Oct. 1957.

63. Donovan, Harvey, and Wade, Phys. Rev. (to be published).

64. Raymond Chastel, Nuclear Evaporation and Temperature, Preliminary Results of the Study of the Spectrum of the Photoprotons from the Reaction Cu (γ,p) Ni, With the Help of a Spectrum of Monochromatic Rays, Compt. rend. 242, 1440-3 (1956). In French.

65. B. T. Feld, H. Feshbach, M. L. Goldberger, H. Goldstein, V. F. Weisskopf, Final Report of the Fast Neutron Data Project, NYO-636, Jan. 1951, p. 115-116.

66. A. P. Vinogradov, I. P. Alimarin, V. I. Baranov, A. K. Lavrukhina, T. V. Baranova, and F. I. Pavlotskaya, in Meetings of the Division of Chemical Sciences, Session of the Academy of Sciences of the U.S.S.R. on Peaceful Uses of Atomic Energy. July 1-5. 1955 (Publishing House of the Academy of Sciences of the U.S.S.R., Moscow, 1955), pp. 85-100.

67. M. L. Goldberger, Phys. Rev. 74, 1269 (1948).

68. K. J. Le Couteur, Proc. Phys. Soc. (London) 63A, 259 (1950).

69. A. A. Ross, Hans Mark, and R. D. Lawson, Phys. Rev. 102, 1613 (1956).

70. S. T. Butler, Phys. Rev. 106, 272 (1957).